Rock descriptions and radiometric dating recomendations for PIP project IS16/04

Carl Stevenson,

University of Birmingham

Edgbaston,

Birmingham B15 2TT

19/10/2017

Contents

List of figures	iii
List of tables	iii
1. Introduction and overview	1
1.1 Radiometric dating: K-Ar and Ar-Ar	3
2. Sample descriptions	4
2.1 Rockall	4
2.1.1) **12/2-1z**	4
- **12/2-1z 3963.6 m (close to base)**	6
- **12/2-1z 3963.0 m (37 cm from base)**	7
- **12/2-1z 3962.81 m**	9
2.1.2) **16/28sb-01**	10
- **16/28-sb01 148.25 m (base)**	11
- **16/28-sb01 147.6 m (top)**	13
2.2 Slyne	14
2.2.1) **19/13-sb02 (BH1A)**	14
2.3 Porcupine	17
2.3.1) **35/8-1**	18
2.3.2) **35/13-1A**	21
2.3.3) **43/13-1**	23
- **43/13-1 2550-2560 m**	24
- **43/13-1 2590-2600 m**	24
2.3.4) **26/30-1**	24
- **26/30-1 5601’**	25
- **26/30-1 5620’**	25
2.4 Goban Spur	26
2.4.1) **62/7-1**	26
2.5 Fastnet	30
2.5.1) **56/26-1**	32
References	34
Appendices	37
- **Appendix 1:** Summary of dating recomendations	37
- **Appendix 2:** List of photomicrographs	39
- **Appendix 3:** Photomicrographs	41

List of Figures

Figure 1: Location map overview map	2
Figure 2: Location map of the Rockall Basin	4
Figure 3: Section of core log for well 12/2-1z	5
Figure 4: Core photos from well 12/2-1z	6
Figure 5: Photomicrographs from 12/2-1z sample from 3693.6 m	7
Figure 6: Photomicrographs from 12/2-1z sample from 3693.0 m	8
Figure 7: Photomicrograph from 12/2-1z sample from 3962.81 m	9
Figure 8: Portion of core log from bottom of well 16/28-sb01	10
Figure 9: Core photos from well 16/28-sb01	11
Figure 10: Photomicrographs from 16/28-sb01 sample from 148.25 m.	12
Figure 11: Photomicrographs from 16/28-sb01 sample from 147.6 m	13
Figure 12: Location map of Slyne and Erris Trough	14
Figure 13: Portion of core log from well 19/13-sb02(BH1A)	15
Figure 14: Photomicrographs of samples from well 19/13-sb02	16
Figure 15: Well locations in the Porcupine Basin	17
Figure 16: Portion of the core log for well 35/8-1	18
Figure 17: Core photos from well 35/8-1	19
Figure 18: Photomicrograph of sample from 35/8-1	20
Figure 19: Portion of core log for well 35/13-1A	21
Figure 20: Photo of core sample from well 35/13-1A	22
Figure 21: Photomicrograph of sample from 35/13-1A	23
Figure 22: Portion of core log for well 43/13-1	23
Figure 23: Portion of core log for well 26/30-1	24
Figure 24: Location and geology of Goban Spur	26
Figure 25: Portion of core log for well 62/7-1	27
Figure 26: Photo of core sample from well 62/7-1	28
Figure 27: Photomicrographs from sample 62/7-1	29
Figure 28: Location map the Fastnet Basin	30
Figure 29: Portions of core logs from three wells from Caston *et al.*, (1981) Fig. 2	31
Figure 30: Core photo and portion of core log from well 56/26-1.	32
Figure 31: Photomicrographs from sample 56/26-1	33

List of Tables

Table 1: Summary of samples in this study	1

1. Introduction and overview

This report provides petrographic descriptions of samples of igneous and volcanic rocks from a selection of wells and intervals have been selected for description and/or radiometric dating as part of PIP (Petroleum Infrastructure Programme) project IS16/04 *An Integrated Biostratigraphic & Lithostratigraphic Framework of Offshore Ireland*. This study was subcontracted to the author by Merlin Energy Resources which is leading the consortium that is carrying out the overall project. Samples were collected by P. Copestake (Merlin Energy Resources) from the PAD core store, Dublin, during June 2017. The author acknowledges the support and assistance of Drs Philip Copestake and Tim Wright of Merlin Energy Resources during the course of this study. All samples, data and reports were provided to the author by Merlin. Comments on a draft of this report were provided by Kara English of the PAD.

The report outlines the area of study and briefly reviews the tectonic context and major igneous events of relevance. A précis of key radiometric techniques proposed is also provided before detailed petrographic descriptions of each samples along with an assessment and recommendation for radiometric dating. The samples studied are tabulated below:-

Well/ Borehole	Penetration type	Number of samples taken for rad dating	Number of samples for description	Sample depths (m)	Sample depths (ft)	Sample type	Basin	Lithology	Known age
12/2-1Z	well	3	3	3962.81, 3963.0 3963.6m	13001.35, 13001.97, 13003.94ft	core	Rockall (Dooish)	Altered basalt	Eocene or Triassic
16/28-sb01	shallow bh	2	2	147.76, 148.25m	484.78, 486.38ft	core	Rockall	Basaltic breccia	Cretaceous
19/13-sb02 (BH1A)	shallow bh		1	106.4m	349.08ft	core	Slyne	Fine grained basalt	Eocene? 54.3 ± 1.2 Ma
35/8-1	well	1	1	3251.61m	10668ft	core	Porcupine	Ash	Albian-Aptian
35/13-1A	well	1	1	3834.208m-3834.218m	12579.42-12579.46ft	core	Porcupine	Gabbro	Oligocene
43/13-1	well	2	2	2550-2560m, 2590-2600m	8366.14-8398.95, 8497.38-8530.18ft	W&D cuttings	Porcupine	Drilling mud and some lava	Palaeocene
62/7-1	well	1	1	2934.31m	9627ft	core	Goban Spur	Porphyritic basalt	Mid Jurassic? 133 Ma
26/30-1	well	1	1	1709.93, 1712.98m	5610ft, 5620ft	W&D cuttings	Porcupine	Drilling mud and some granite	275 Ma, 290 Ma Variscan
56/26-1	well	1	1	2930.55m	9614.67ft	core	Fastnet	Gabbro	K-Ar 170 Ma

Table 1: Summary of samples used in this study

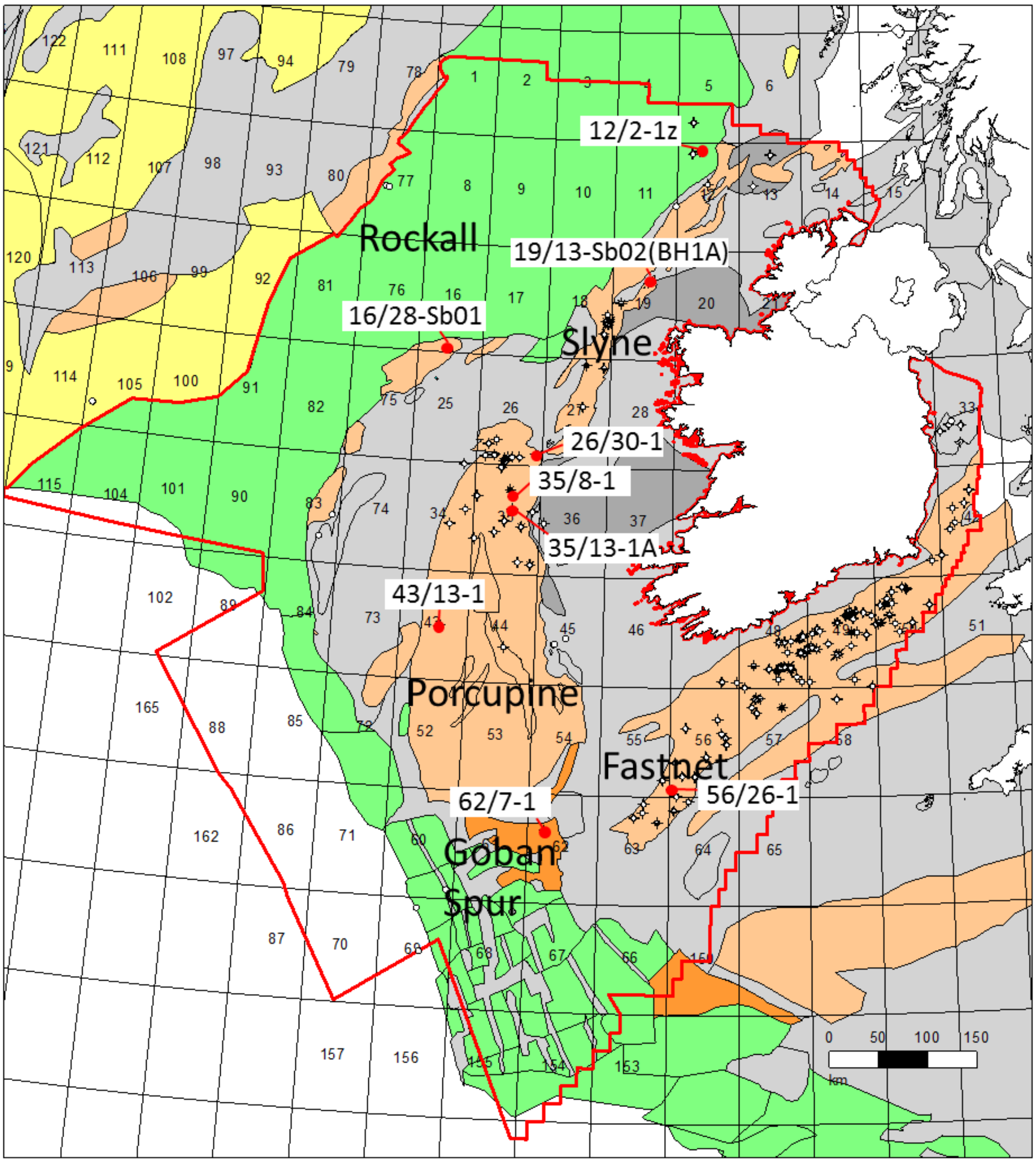

Fig. 1: Overview location map. Outlines of key basins with names of basins relevant to this study. All wells and boreholes in the region are marked. Samples used in this study are highlighted with the well name indicated.

The continental shelf offshore Ireland is comprised of a number of isolated but tectonically linked mainly clastic basins that developed on Proterozoic basement throughout the Phanerozoic leading ultimately to North Atlantic spreading in the early Cenozoic (Shannon, 1991; Doré *et al.*, 1999; Naylor and Shannon, 2005; Funck *et al.*, 2016; Stoker *et al.*, 2016). Extensional basin formation throughout post Caledonian convergence was tectonically linked by pre-Caledonian and Caledonide basement structure and forms a single passive margin. Post-Variscan Carboniferous tectonic collapse and subsidence were poorly preserved having been overprinted by younger extensional events. Key extensional phases were experienced in; 1) Permo-Triassic, 2) Early Jurassic, 3) Late Jurassic-Early Cretaceous, 4) Late Cretaceous and 5) Late Eocene. Basement structures exerted a significant control on basin formation as well as providing conduits for Mesozoic and Cenozoic magmatism (Naylor and Shannon, 2005).

Volcanics and intrusions are penetrated by wells throughout the area. Available timing constraints and dating indicate magmatic events in Triassic, Middle Jurassic, Early Cretaceous and Eocene.

1.1 Radiometric dating: K-Ar and Ar-Ar

For detailed review of Ar-Ar and K-Ar thermochronology, the reader is referred to Kelley (2002). The sample suite from the current study may be dated using either K-Ar or Ar-Ar techniques. The K-Ar technique relies on the decay of ^{40}K to ^{40}Ar with a half-life of 1.248 x 10^{-9}. The long half-life makes this technique suitable for rocks older than 100,000 ya up to a few Ga. Although the technique is well suited to a range of rock types due to the abundance of K in several common rock forming minerals, the main limitation is the reliance on the blocking of Ar loss below 300°C. Below this temperature, ^{40}Ar accumulates according to the decay constant which means that the amount of Ar is affected by subsequent hydrothermal or metamorphic events. Therefore, any ages determined from a rock or mineral that has experienced temperatures above the blocking temperature will be either partially or totally reset by the younger thermal event. In addition, other minerals may form during these events meaning that the samples must be as unaffected as possible by subsequent thermal events to determine a representative age . Alteration can to some extent be mitigated by separating and dating single crystals of a particular phase in a mineral separate, but Ar loss may occur due to >300°C thermal events. Thus, interpretation of K-Ar dates from slightly altered or metamorphosed lithologies need to bear in mind this potential Ar loss and be aware that dates may reflect a mixture of different thermal events.

The Ar-Ar technique is an improved version of K-Ar. Whereas the former relies on a direct measurement of K and Ar separately, the latter uses the ^{39}Ar-^{40}Ar ratio from a sample that has been irradiated causing ^{39}K to produce ^{39}Ar proportional to the K content. This allows more precise measurements only requiring measurement of Ar in the same sample. The date from Ar-Ar is calculated based on a sample of known age. Step heating also allows the excess Ar or Ar loss to be identified revealing multiple ages from one sample including the initial crystallisation age and subsequent thermal events.

The ability to date younger metamorphism or hydrothermal events from Ar-Ar dating provides added value to dating by contributing to basin history analyses. Further still, it may be possible to correlate the age of hydrothermal or heating events with intrusion or volcanic events elsewhere in the record. However, the need to irradiate samples for Ar-Ar dating and to subsequently allow several months for the sample to cool, means that the Ar-Ar method includes a much higher cost compared to K-Ar and longer time required to carry out the analysis.

2. Sample descriptions

2.1 Rockall

The Rockall basin extends from the Northern Rockall-Hebrides Margin to the South Rockall-Porcupine Margin (Stoker *et al.*, 2016). In the area of interest, the basin is flanked to the NW by the Hatton Bank and to the SE by a series of perched basins in the NW of the Porcupine High (Fig. 2). The main phase of extension in the Rockall basin was Late Jurassic to Mid Cretaceous. Igneous activity in Rockall is mainly Mesozoic lavas and Palaeogene intrusions. Two wellbores from Rockall are included in this study; 12/2-1z (Dooish) to the north of the Erris Basin and 16/28sb-01 from the N end of the Macdara Basin on the NW flank of the Porcupine High (Fig. 2).

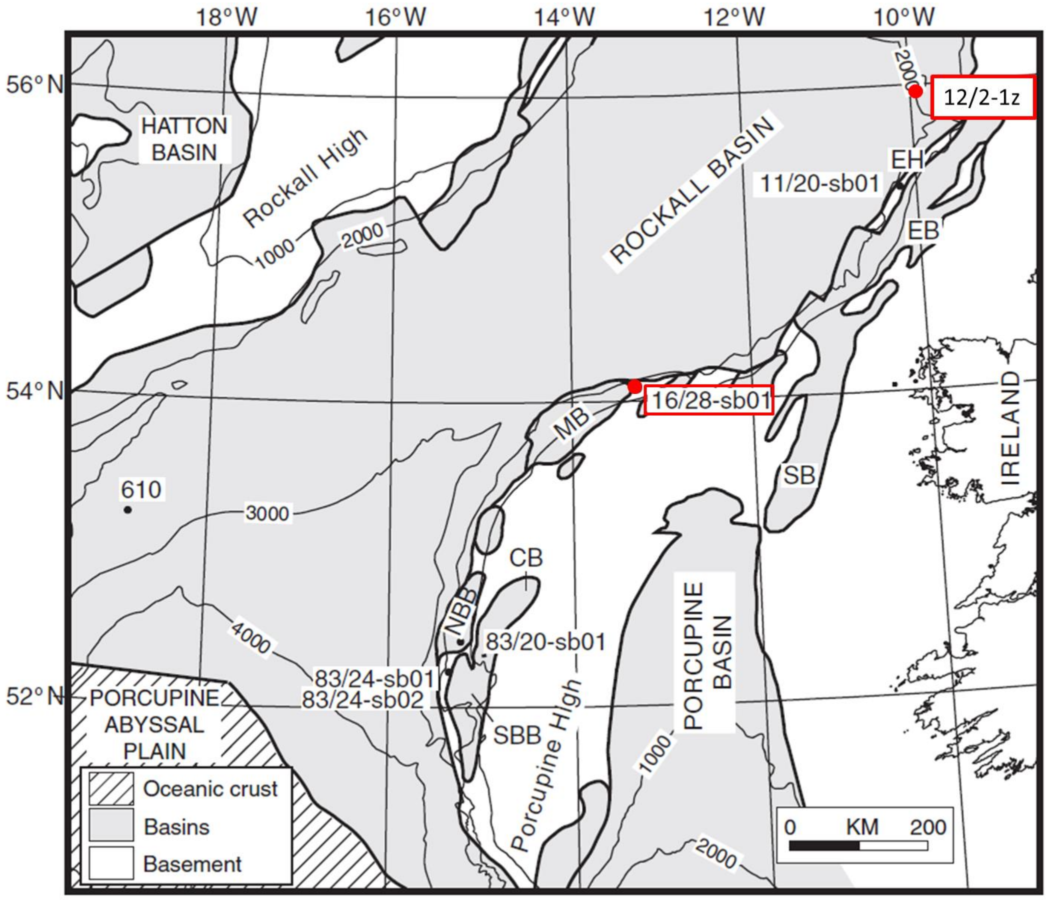

Fig. 2: Map of the Rockall Basin showing major basin structure and location of wells in this study. Adapted from Haughton *et al.* (2005) with the inclusion of well 12/2-1z. Acronyms for sub-basins can be found in Haughton *et al.* (2005) but relevant to this study, MB = Macdara Basin.

2.1.1) **12/2-1z**

12/2-1z was a side track of well 12/2-1 drilled to test the Dooish prospect. The final well report noted an extrusive at 3950.55-3956.25 m. This study has sampled at 3962.81 m and 3963.0 m (core depth) (3958.18-3963.37 m MD) near the base of the extrusives (Fig. 3). The age of this basalt is ambiguous. The initial Shell report stated a K-Ar age of 250 Ma [Early Triassic], but this was later ruled out with an Eocene Ar-Ar age and interpreted to be an intrusion into soft sediments above harder pre-rift section.

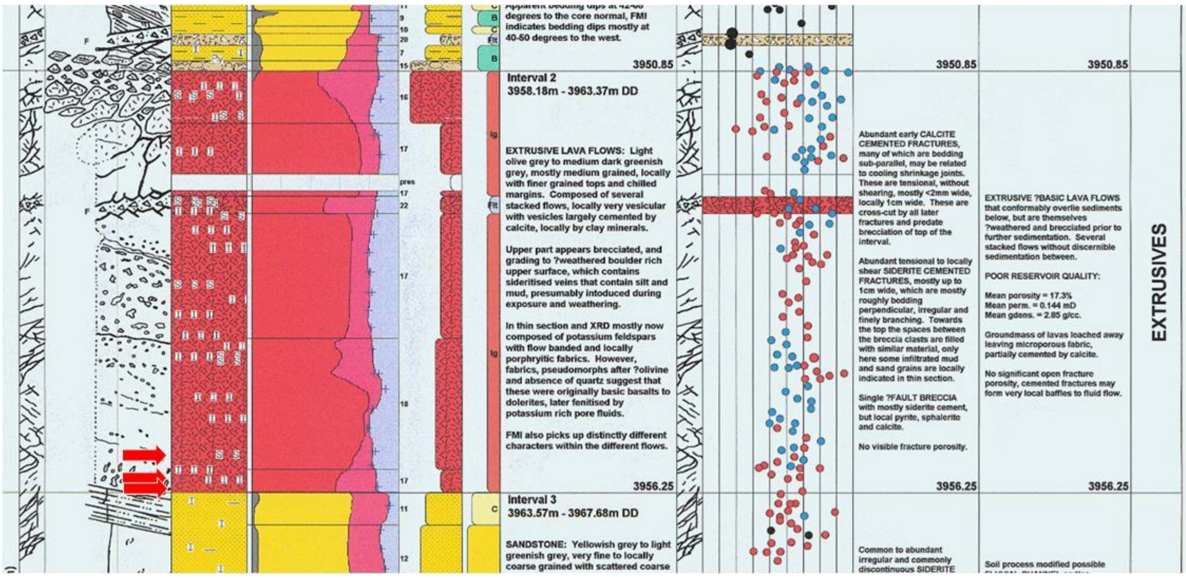

Fig. 3: Core log for well 12/2-1z from the Robertson sedimentological log by Lucas (2004). Red arrows indicate the position of samples used in this study.

Core photographs (Fig. 4) seem to suggest soft sediment deformation sub basalt, but this appears to be tectonically driven slope failure as opposed to lava or volcanic related. Anything approaching apparent pepperitic textures are below ca. 4000 m and described as slightly flattened calcite nodules. The pale colour of these nodules is more likely to be calcite than altered igneous material. The base of the lava shows amygdales filled with apparent zeolites and a sharp conformable contact with sandstone. Sediment directly in contact with lava base may be hornfelsed obscuring soft sedimentary textures.

Figure 4 shows the top of the lava to be vesicular and appears to be brecciated in contact with overlying sediment. This seems to be reworking of lava into the sediment. Subangular fragments of lava containing pre-entrainment veins suggest that this is erosion of cooled basalt as opposed to interaction of hot lava and wet sediment.

There does not seem to be intrusion into soft sediment at the top or bottom of the lava. However, alteration is pervasive and not apparently associated with fractures. The alteration is possibly due to emplacement into water/wet sediment and related metasomatism by meteoric/sea water during or soon after emplacement, as opposed to subsequent high temperature hydrothermal alteration due to lava-sediment interaction.

Lithified sediments around an intrusion may be disrupted or fluidised by hydrothermal fluids generated by the intrusion of hot magma (Schofield *et al.*, 2010, 2012). This may explain some breccia like features in this core and may therefore allow for a younger than expected radiometric date. However, pre-entrainment veins and fragments of lava in the breccia tend to argue against this interpretation.

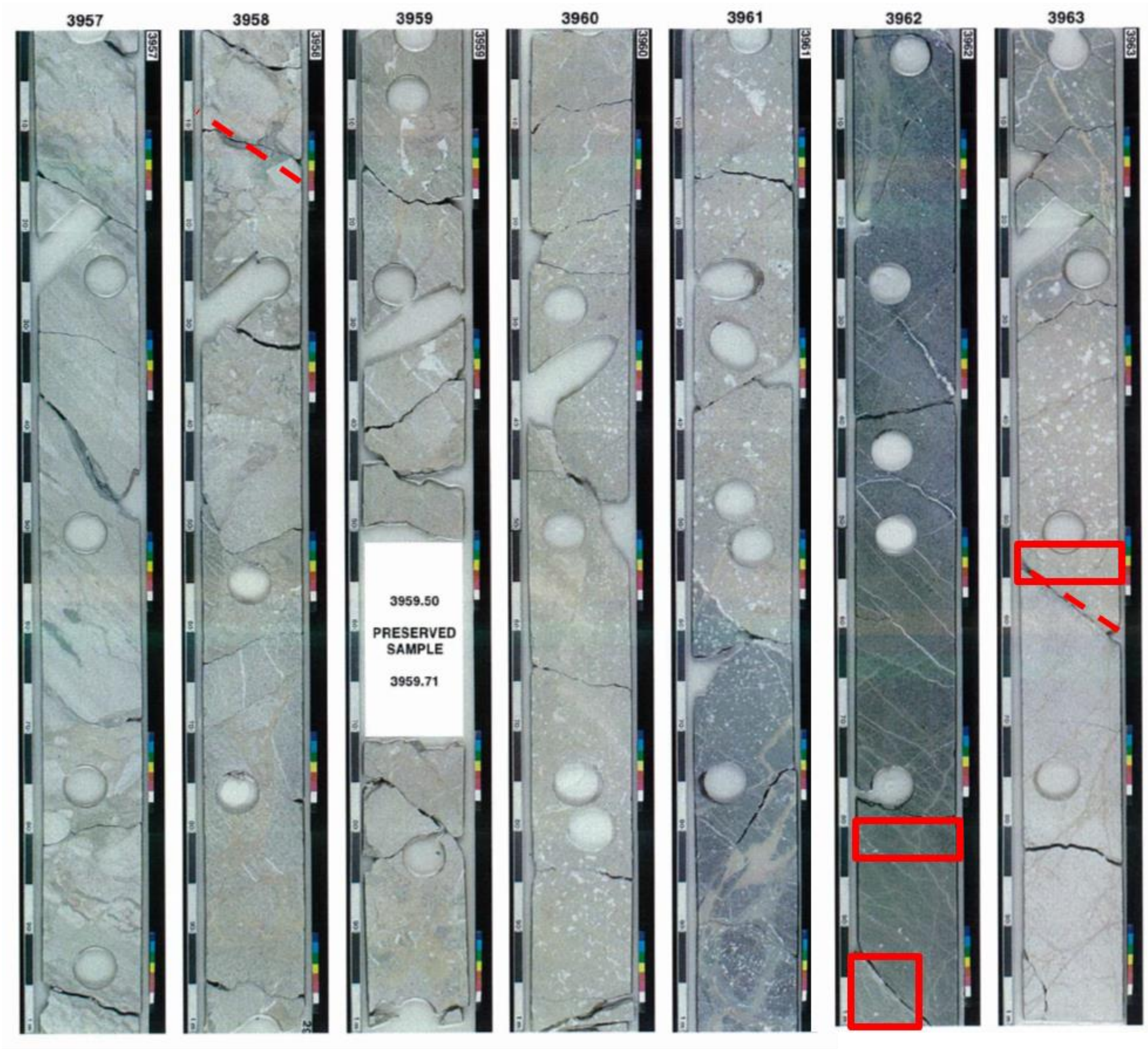

Fig. 4: Core photos of cores from well 12/2-1z. Red boxes indicate three samples taken for this study near the base of the basalt. Red dashed lines at 3958.1 m and 3963.3 m are the top of the basalt and bottom respectively, based on Robertson sedimentological log by Lucas (2004), see Fig. 3.

- **12/2-1z 3963.6 m (close to base)**

Sample is pale green, highly altered amygdaloidal basalt. Dominant texture is a fine grained, chlorite and epidote dominated matrix (groundmass) with 2-5 mm rounded, circular to irregular amygdales or white sparry calcite. Occasional brownish orange staining on fracture surfaces, but veining is sparse to absent.

Thin section:

Thin section shows a heavily argillised groundmass with amygdales filled mainly with coarse spar calcite (Fig. 5). Amygdale fills are occasionally composite with a finer grained carbonate showing some browning staining between crystals. There is a gradational contact between the finer amygdale fill and the coarser (1-2 mm calcite crystals) fill. Feldspar is present in the groundmass with interstitial clays. Feldspar shows simple Carlsbad twining, indicating potassium feldspar (consistent with report from sample at 3963.5 m) (Fig. 5B). This is likely metasomatic replacement of plagioclase and as such probably happened during emplacement into aqueous (likely marine) environment or very soon after.

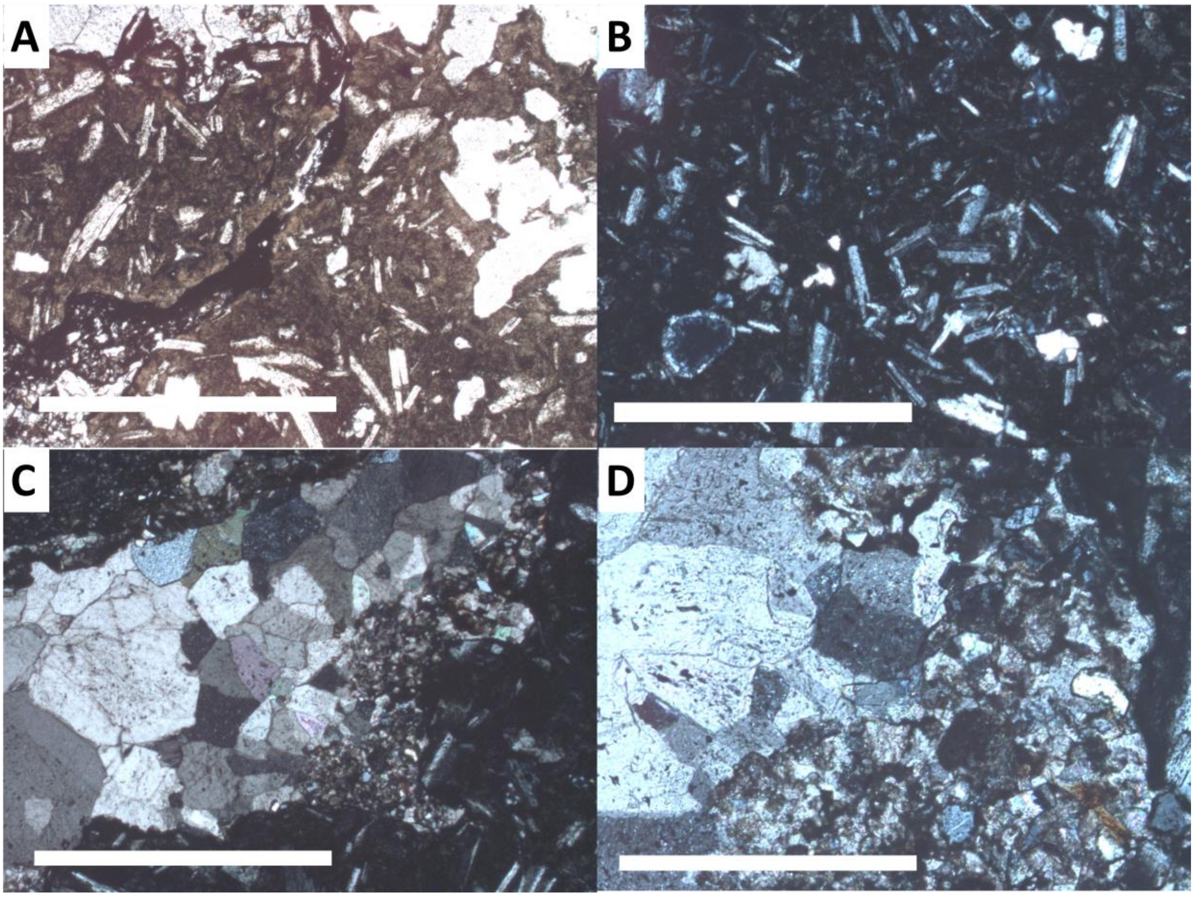

Fig. 5: Photomicrographs from 12/2-1z at 3693.6 m. A) Plane polarised light, scale bar is 4 mm. Dominant texture is large rounded but irregular inclusions surrounded by a matrix of mainly altered (greenish chlorite and undifferentiated clays) groundmass and euhedral <1 mm laths of feldspar. B) In cross polarised light, feldspars are mainly potassium feldspar (identified though simple Carlsbad twinning). Scale bar = 4 mm. C) Cross polarised light, scale bar = 4 mm. Composite fill of inclusions. These are likely amygdales filled mainly with coarse crystalline calcite. Occasionally on one side the inclusion fill gives way to finer grained mix of calcite, clay and needles of zeolite. D) Crossed polarised light, scale bar = 1 mm. Detail of finer grained inclusion fill.

Dating recommendation: This is the most likely from the three samples taken from this well to yield a crystallisation (or at least alteration soon after emplacement) age. The sample is pervasively altered and potassium feldspar is likely metasomatic alteration of plagioclase. Ar-Ar on a feldspar mineral separate recommended.

- **12/2-1z 3963.0 m (37 cm from base)**

Sample appears to be a pale green, highly altered basalt. Thin (~1 mm) sparse veins of coppery/orange (cuprite, siderite?) cut similarly thin and sparse white calcite veins.

Thin section:

In thin section, the sample is extensively altered (Fig. 6). Mineralogy is dominated by calcite, clay minerals, opaques and some minor zeolites (Figs. 6A & B). There are no primary igneous phases remaining and any primary igneous texture seems to have been almost completely overprinted. Ca. 1 mm thick veins show at least three phases of hydrothermal activity: 1) very fine dark red (PPL), 2) sparry calcite 3) slightly coarser dark red (PPL) with some zeolite and fragments of vein 2 (Fig. 6D).

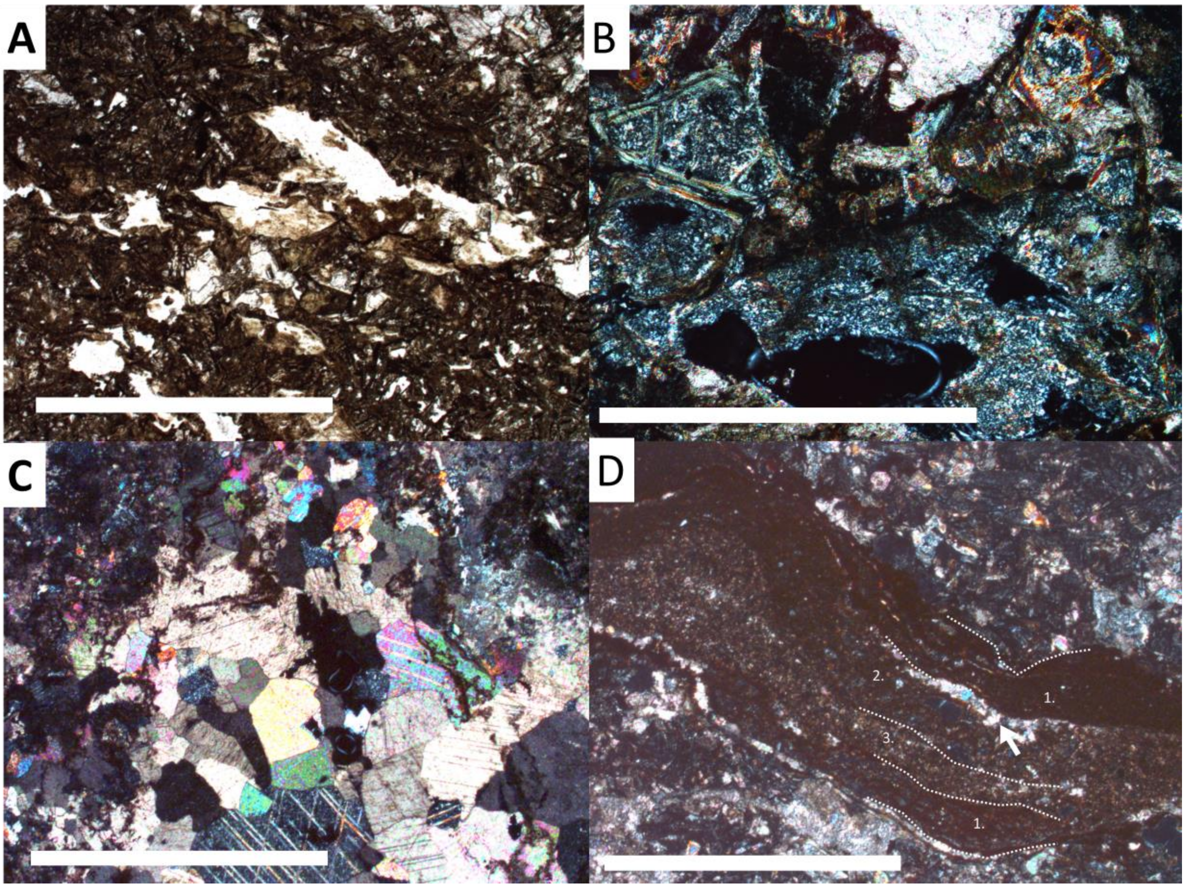

Fig. 6: Photomicrographs from sample 12/2-1z 3963.0 m. A) Plane polarised light, scale bar = 2 mm. Greenish brown sericitisation and chlorite dominating groundmass. B) Crossed polarised light, scale bar = 1 mm. Micro sphericular zeolite dominates view and mainly replaces primary igneous minerals. Calcite is present (top middle) and fibrous serpentinite veins remain where olivine has been replaced by zeolite and iddingsite. C) Crossed polarised light, scale bar = 2 mm. Sparry calcite replacing much of the rock. D) Plane polarised light, scale bar = 2 mm. Fine grained material in a vein is opaque and calcite. Multiple stages of vein growth (fine dotted lines and numbers) indicate multiple phases of hydrothermal fluid flow. White arrow highlights a fragment of calcite captured during early vein formation indicating early pervasive replacement alteration before veining.

Calcite forms in irregular/amorphous 1 mm wide clots of sparry calcite (Fig. 6C). These may be replacing phenocrysts or amygdales. Typical calcite crystal size of ~0.3 mm. These are surrounded by a groundmass of undifferentiated calcite, clay, and opaques.

Opaques generally form strongly acicular ~0.3 mm long needles and restricted to the groundmass. They occasionally form more equant ~0.1 mm crystal in clusters around relict phenocrysts.

Zeolites seem to form in pseudomorphing clusters after what look like phenocrysts of amphibole and possibly pyroxene. These relict pseudomorphs show an early fibrous and strongly birefringent, non pleochroic zeolite (possibly stilbite) or clay followed by more prevalent, weakly sphericular and botryoidal, low birefringent and nonpleochroic zeolite (possibly chabsite).

Core report mentions feldspars altered to K-feldspar. This is consistent with metasomatic reactions associated with lava emplaced into aqueous or marine environment.

Dating recommendation: Extensively to complete alteration. This sample is unlikely to yield a reliable crystallisation age. Previous dates must be regarded with caution. Stratigraphic association is the best way to date this horizon. No dating recommended.

- **12/2-1z 3962.81 m**

Sample in a number of pieces. Green with reddish brown minerals (iddingsite possibly replacing olivine). Medium grained, secondary epidote, chlorite, other clays and zeolites are present. Appears to be extensively hydrothermally altered with what might be Cu mineral veins (possibly cuprite), possibly volcanic related.

Thin section:

Extensively altered with no primary phases remaining. Can still see pseudomorphed texture with relict feldspar laths now replaced by clay (sericite). Olivine replaced variously by mica and zeolite occasionally with opaque (c. 0.1 mm thick) rims. Amygdales and irregular cavities occupied by Si zeolite and calcite (former with mica/clay rim). Brownish to opaque staining (iddingsite) seems to be associated with replaced olivine where the relict serpentinite fractures are replaced by opaque (magnetite or haematite) oxide. XRF from Core report suggests hematite, however if this is related to serpentinisation of olivine it may be magnetite. Low magnetic susceptibility would rule out latter.

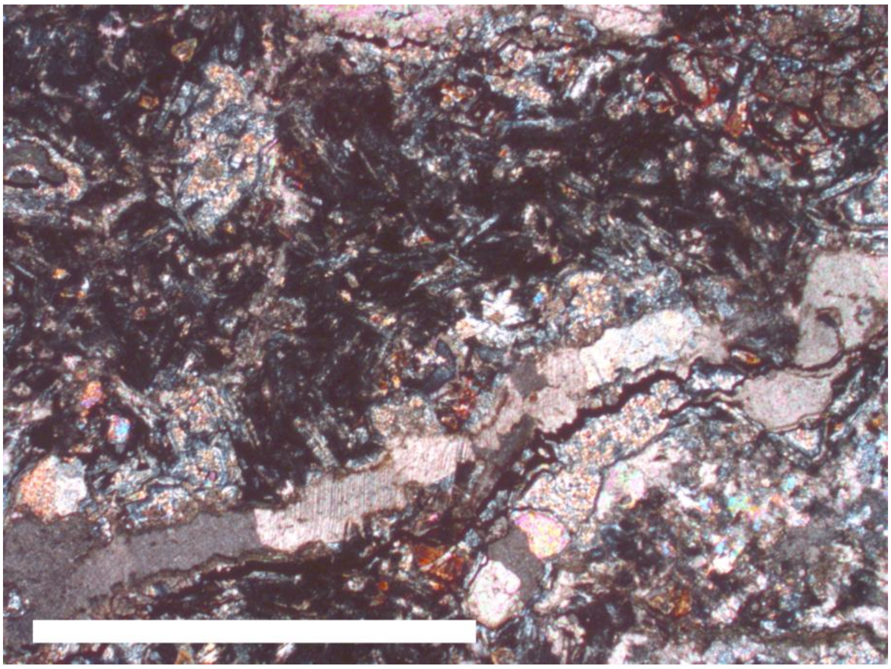

Fig. 7: Photomicrograph from sample 12/2-1z 3962.81 m in crossed polarised light. Scale bar is 2 mm. Replacement of primary minerals by zeolite, clay and opaque minerals and calcite veining.

Dating recommendation: Extensive to complete alteration. This sample is unlikely to yield a reliable crystallisation age. Previous dates must be regarded with caution. Stratigraphic association is the best way to date this horizon. No dating recommended.

2.1.2) **16/28sb-01**

16/28sb-01 is located on the northern flank of the Porcupine high and at the NE end of the Macdara sub basin (Fig. 2). Haughton *et al.* (2005) reported that well 16/28sb-01 penetrated 0.95 m of basalt at 147.30–148.25 m (Fig. 8). This study has sampled this basalt at 147.76 m (ca. 26 cm from the top) and at 148.25 m (at the base). Haughton *et al.* (2005) concluded that the basalt was intra-Cretaceous and linked to the nearby Drol Igneous Centre, although no radiometric dating has been carried out to demonstrate this. In this core, the basalt is unconformably overlain by ca. 2-3 m Cretaceous sandstone. This is overlain by Lower Eocene which on seismic appears to downlap on the top Cretaceous (Haughton *et al.*, 2005). The basalt overlies an intra Cretaceous unconformity that drapes Cretaceous rifting.

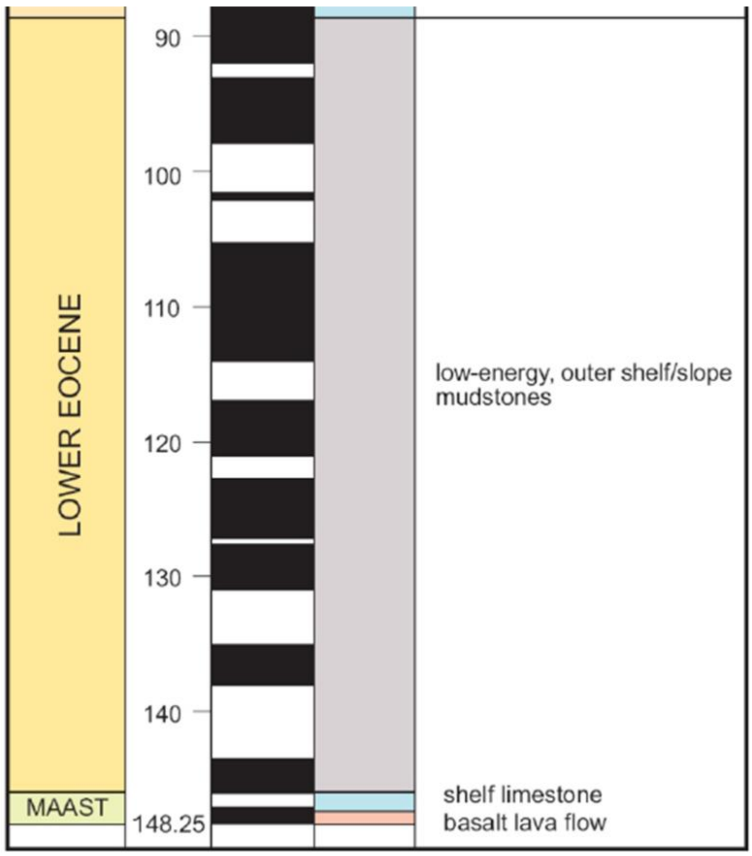

Fig. 8: Portion of core log from bottom of well 16/28-sb01. Source PIP.

Core photographs show the basalt to be moderately veined with pale, presumably calcite, veins that exhibit a yellow-green aureole. Basalt is dark and weakly porphyritic (mainly aphyric) and with sparse amygdales. The core samples appear to have a brecciated texture with inclusions (possibly xenoliths). Alterations seems moderate to extensive but is uneven.

This largely agrees with the core description of Haughton *et al.* (2005):-

> *'The core comprises dark grey to grey-green, aphyric, sparingly vesicular basalt cut by a complex array of inclined and subhorizontal fractures that are sealed by oxide, chlorite, zeolite and carbonate-filled veins and flanked by alteration fronts. Away from the fractures, the fresher basalt appears massive with no evidence for brecciation or obvious pillowing. In thin section (Fig. 10d), the basalt comprises weakly to strongly flow aligned plagioclase laths (that are extensively albitised) and olivine pseudomorphs (now chlorite and iddingsite) set in a groundmass of microcrystalline pyroxene, plagioclase and opaque grains (partly replaced by zeolites) with scattered amygdales (filled by chlorite, zeolite and carbonate).'*

The BGS collected four samples from this core at 147.06-147.76 m, 147.76-147.56 m, 148.10-148.18 m, and 147.76-148.25 m. Samples 147.06-147.76 m and 147.76-148.25 m (top and base of the basalt respectively), were sent for Ar-Ar analysis, but the results of this are unknown at this time (see table 1 in Chambers *et al.*, 2005). Thin section descriptions in this report are similar to those of this study (see Chambers *et al.*, 2005 for further details).

- **16/28-sb01 148.25 m (base)**

Sample is a dark coloured breccia with fine grained, holocrystalline aphanitic matrix (Fig. 9B). Numerous small and subrounded inclusions (xenoliths) are present. These are mainly very fine grained, greenish, 4-6 mm and usually elongate. Also larger (bigger than sample) xenoliths bordered by a (what looks like) white (calcite, zeolite?) vein. The larger xenolith is mantled by a darker possibly chilled margin.

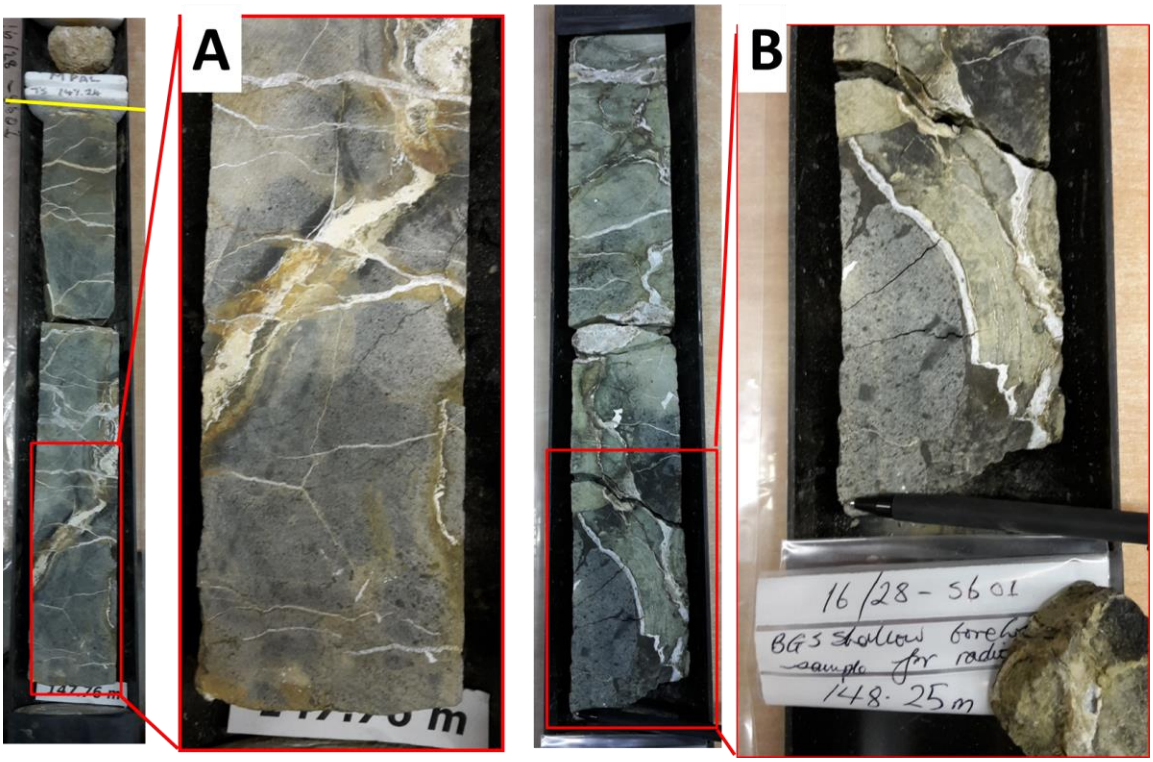

Fig. 9: Core photos of 16/28-sb01 showing samples (red boxes) taken for this study at (A) 147.6 m and (B) 148.25 m. Photos provided by P. Copestake (June 2017). Yellow line is the top of the basalt.

This sample appears to be a basaltic breccia. Possibly erupted into wet sediment, shallow fluvial/marine or part of a hyaloclastite. Basaltic parts look fresh.

Thin section:

Mainly fine grained porphyritic moderately-strongly and pervasively altered basalt (Fig. 10). Plagioclase laths c. 0.5-0.7 mm long phenocrysts aligned in weakly trachytic texture in a groundmass of <0.1 mm plagioclase, quartz and clinopyroxene (Fig. 9A). Plagioclase in this sample is slightly altered but not quite as altered as Haughton *et al.* (2005) indicated. Olivine has been completely replaced and pseudomorphed by brownish green chlorite (Fig. 10C). Sparse amygdales are filled with calcite some kind of microspheroidal Si zeolite, which exhibit patches of orange (Fe?) staining and a halo of similar staining (Figs. 10A & D). Larger pseudomorphs of a fibrous zeolite after pyroxene or amphibole are also present.

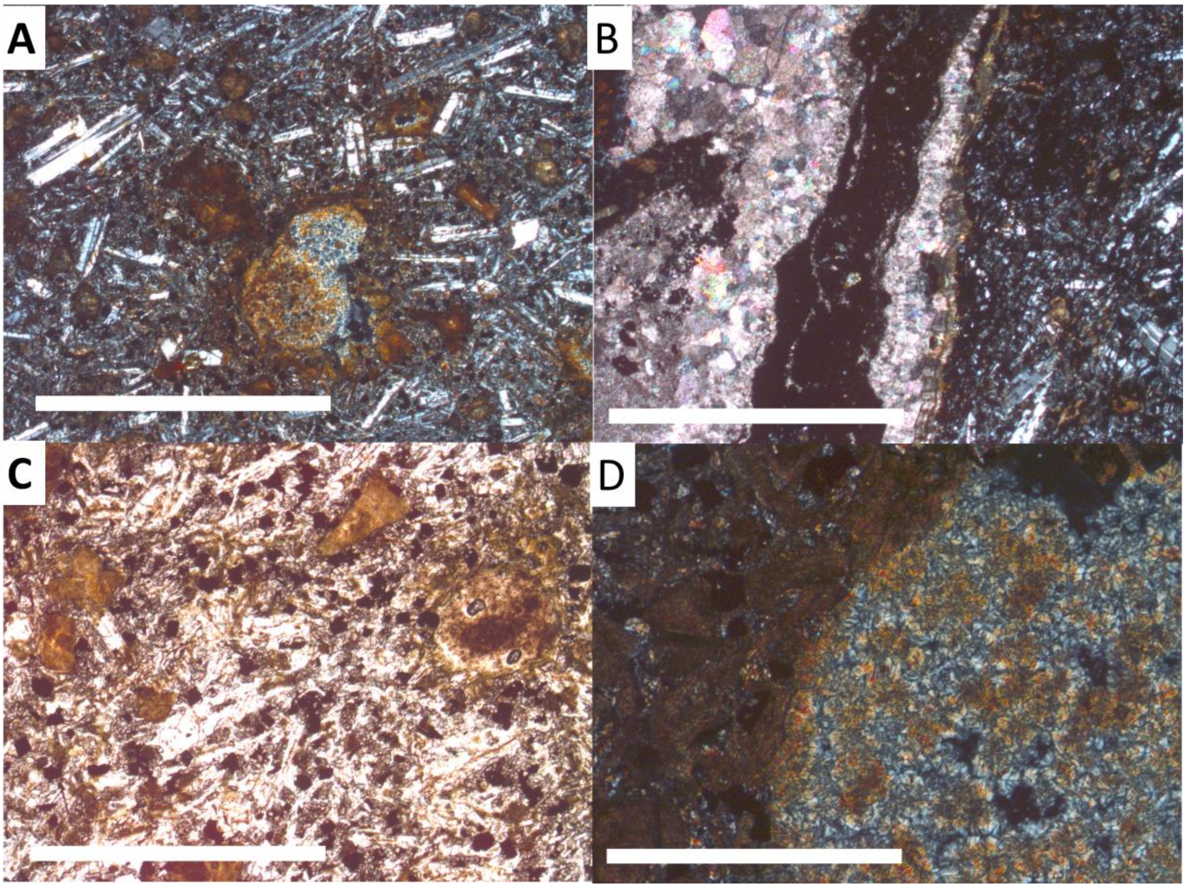

Fig. 10: Photomicrographs from sample 16/28-sb01 148.25 m. A) Plane polarised light, scale bar= 2 mm. Dominant texture is of porphyritic plagioclase laths in a moderately altered groundmass. Amygdales filled by microspheroidal zeolite are patchily affected by and surrounded by an aureole of brown staining. B) Crossed polarised light, scale bar = 2 mm. Detail of a vein showing early sparry calcite followed by opaque vein fill. C) Plane polarised light, scale bar = 2 mm. Similar texture to (A) but in PPL, oxides are more apparent and seem to be primary and olivine replaced by greenish chlorite. D) Crossed polarised light, scale bar 0.5 mm. Detail of microspheroidal zeolite filling amygdales.

Veins of calcite and opaque (oxides) show multiple phase of late fluid flow (Fig. 9B). These veins cut amygdales. Feldspars also appear fractured. Groundmass in patches close to larger veins pervaded by fractures filled with oxides. Groundmass is pervasively altered but feldspars, although fractured, seem fresh enough.

Dating recommendation:

Altered ground mass and weakly altered plagioclase phenocrysts should be separately dated using Ar-Ar.

- **16/28-sb01 147.6 m (top)**

Sample appears moderately veined with 1-4 mm thick white (calcite or zeolite) veins (Fig. 9A). Veins are flanked by paler (alteration) rock. Away from veins but in patches are darker, fine grained but apparently holocrystalline, possibly primary basaltic rock.

Thin section:

Very similar to the 148.25 m sample.

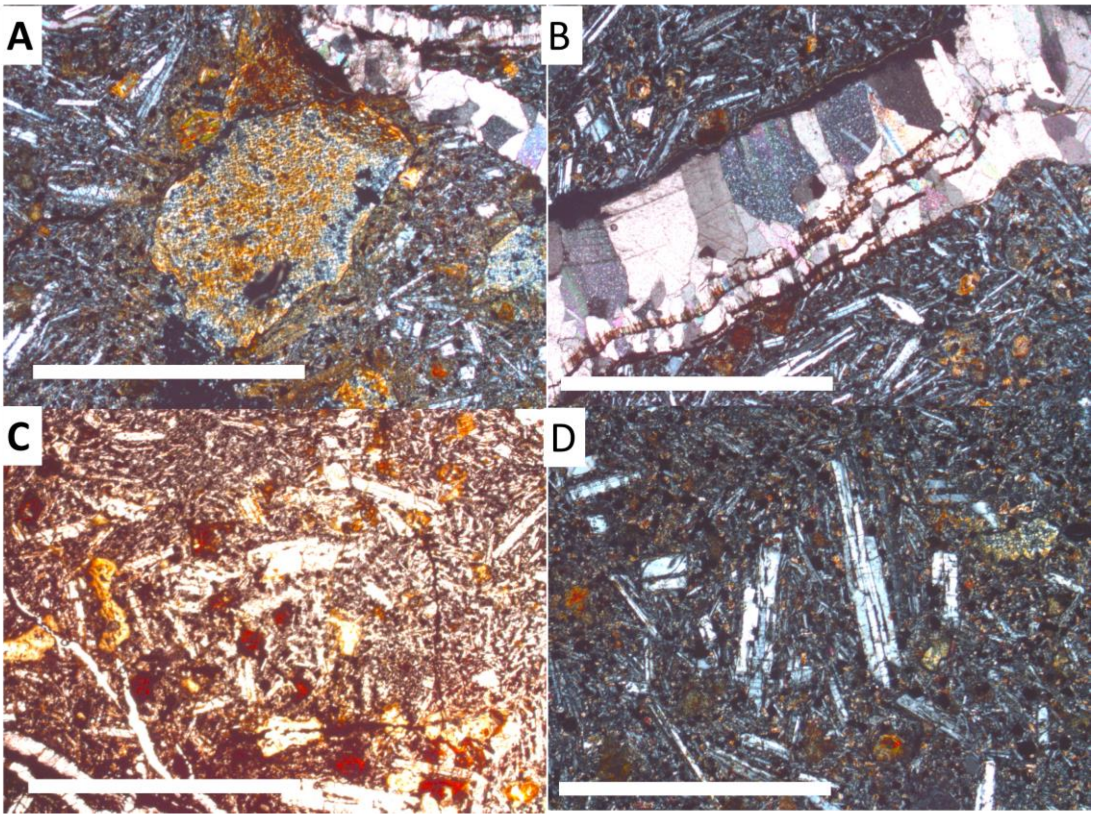

Fig 11: Photomicrographs of sample 16/28-sb01 147.6 m. A) Crossed polarised light, scale bar =2 mm. Larger cavity (amygdale or miarolitic) filled with zeolite showing orange staining and aureole. Sparry calcite vein fill also present (top right). B) Crossed Polarised light, scale bar = 1.5 mm. Detail of calcite vein showing multiple phased of vein growth indicating multiple fluid flow events. C) Plane polarised light, scale bar = 2 mm. Red (oxyhydroxide) secondary minerals present. D) Crossed polarised light, scale bar = 2 mm. Porphyritic texture and secondary minerals.

Dating recommendation:

Altered ground mass and weakly altered plagioclase phenocrysts should be separately dated using Ar-Ar.

2.2 Slyne

The Slyne Basin is a NNE trending Mesozoic half-graben that extends for the northern end of the Porcupine Basin to the Erris Basin and northern Rockall Trough (Dancer *et al.*, 1999). Extension in the Slyne Basin began in the Permo-Triassic but the main phase was Middle Jurassic. Eocene volcanics in the Slyne Basin and Malin Shelf consist of basaltic lavas, tuffs and ignimbrites that have been dated as 40-43 Ma in well 18/20-1 (Dancer *et al.*, 1999). This study has sampled core from well 19/13-sb02 (BH1A).

2.2.1) **19/13-sb02 (BH1A)**

This study has sampled basalts from well 19/13-sb02 (BH1A) at 106.4 m in an offshoot of the Northern Slyne Basin (Fig. 12). A K-Ar date of 54.3 ± 1.2 Ma was determined by Statoil from 107.22 m in this well. However, the report acknowledges weathering of the groundmass and likely Ar loss. This date is therefore a minimum age of eruption and likely affected by younger alteration. This is not likely to be a reliable date.

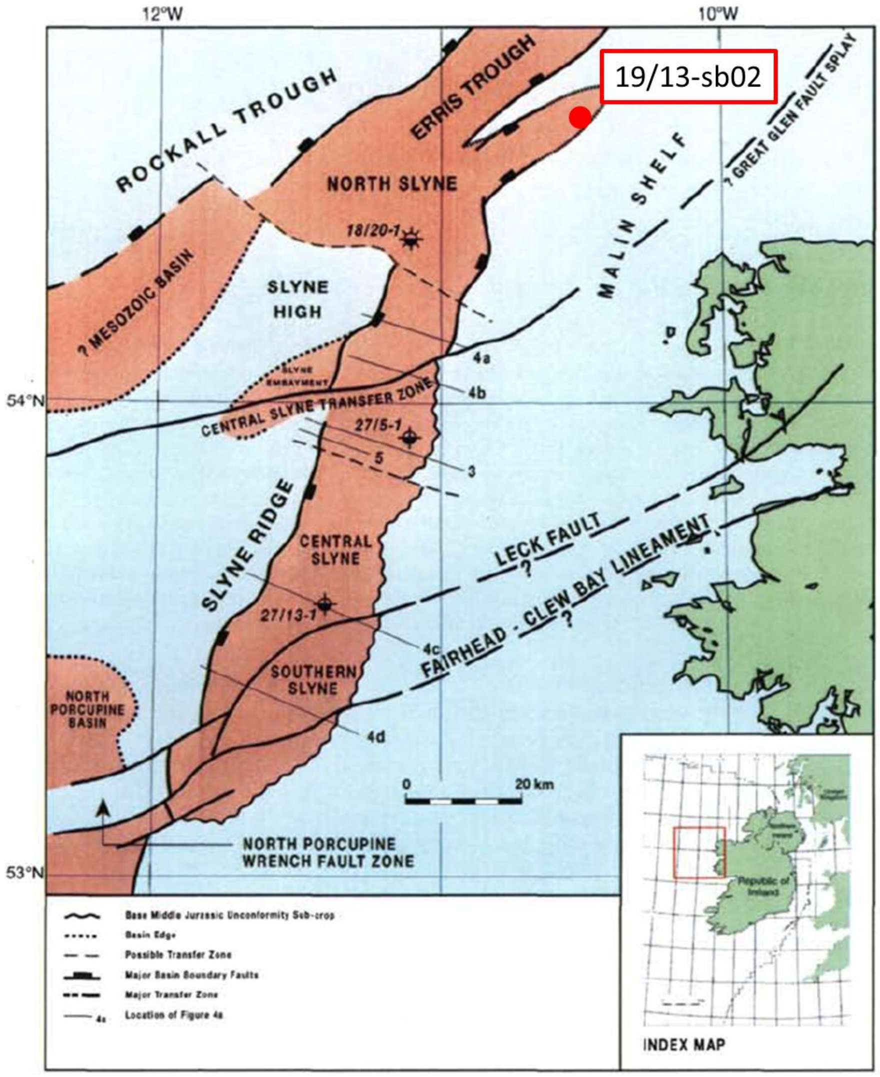

Fig. 12: Location of well 19/13-sb02 adapted from Dancer *et al.* (1999) with addition of 19/13-sb02 from well report.

Basalt lavas were penetrated at 95-112.5 m and are overlain by Pliocene sands and gravels (Fig. 13). The BGS sampled this core at 109-109.15 m and sent this sample for Ar-Ar analysis (Chambers *et al.*, 2005). However, the results of this analysis are unavailable at this time.

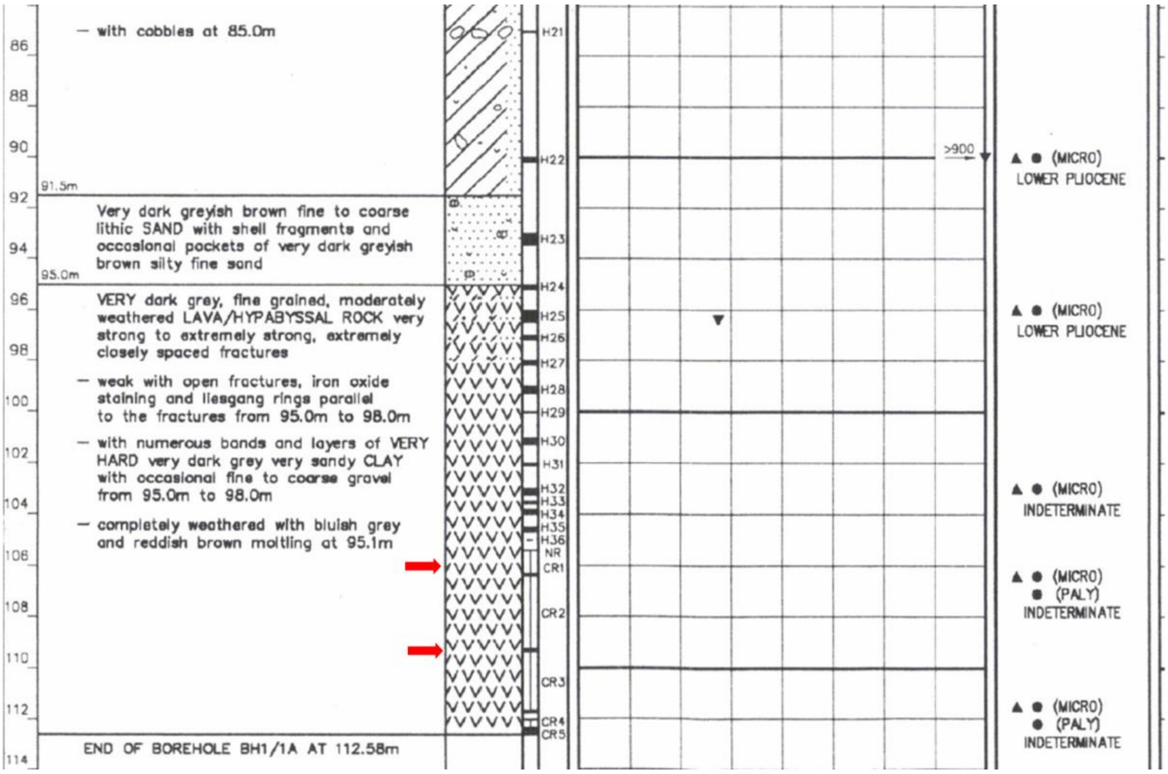

Fig. 13: Core log from well 19/13-sb02 (BH1A). Red arrows show sample from this study (upper) and location of date derived from Shell sampling in well report (lower).

Sample appears dark and very fine grained, aphanitic almost glassy basalt. Too fine grained to identify much in hand specimen. Some patches of green and brown staining indicate some minor secondary alteration.

Thin section:

Fine grained slightly altered basalt. Dominated by plagioclase and some fine clinopyroxene and opaques (Fig. 14). Patchy variously greenish (bowlingite [saponite] according to Chambers *et al.*, 2005) and reddish staining. Reddish mineral sparsely present is possibly a Mn rich epidote or oxyhydroxide. Chambers et al (2005) refer to a pilotaxitic fabric that is also evident in this sample.

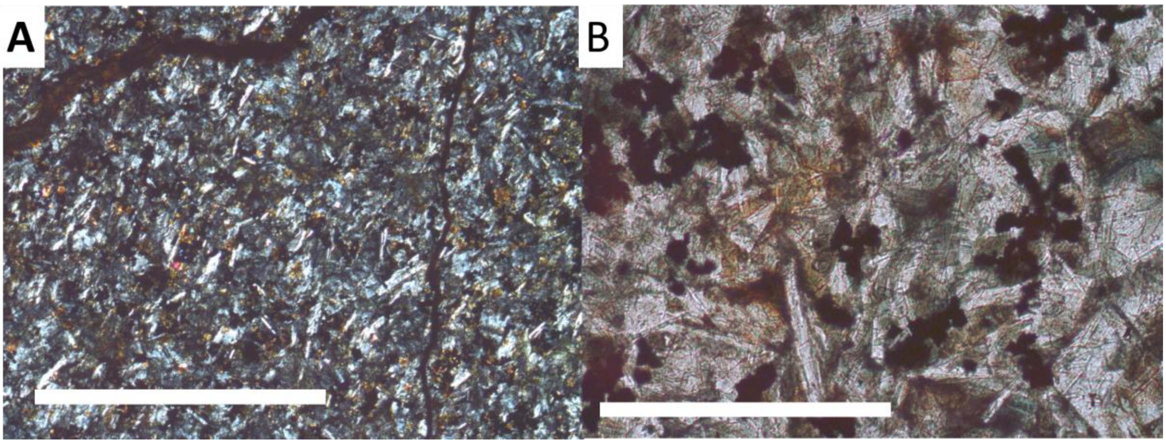

Fig. 14: Photomicrographs from sample 19/13-sb02. A) Crosses polarised light, scale bar = 1 mm. Fine grained plagioclase and ferromagnesians with moderate sericitisation and veining. B) Plane polarised light, scale bar = 0.2 mm. Opaques interstitial to plagioclase but seem primary. Some patchy and subtle greenish (chloritic) and brown (Fe) staining is present, also scattered isolated needles of likely zeolite.

Dating recommendation:

Alteration looks worse in thin section but is moderate at worst. Too fine grained to separate phases so whole rock analysis may be required for dating by Ar-Ar.

2.3 Porcupine

The Porcupine Basin is a large, north-south trending basin ca. 200 km SW of Ireland (Fig. 15). Similar to most Irish offshore basins, rifting began in the Permo-Triassic with major rifting in the Jurassic and younger minor rifting in the Cretaceous (Tate, 1993; Shannon *et al.*, 1991) except that it records extreme extension with stretching factors up to 6 (Reston *et al.*, 2004). Volcanics are present in the Triassic (North Porcupine), throughout the Lower Cretaceous and the Lower (Palaeocene) and Middle (Oligocene) Cenozoic (Tate, 1993). Some controversy exists over the origin of a subsurface feature identified in wide-angle seismic and coincides with a free air gravity anomaly called the Porcupine Arch (Naylor *et al.*, 2002). This feature has been variously interpreted as volcanic (Tate, 1993; Calvès *et al.*, 2012), serpentinite mud volcano (Reston *et al.*, 2001, 2004) or a rotated fault block (O'Sullivan *et al.*, 2010).

This project has provided core samples from wells 35/8-1 and 35/13-1A and cuttings from 43/13-1 and 26/30-1. These samples should capture Lower Cretaceous and Cenozoic magmatic events (Fig. 15).

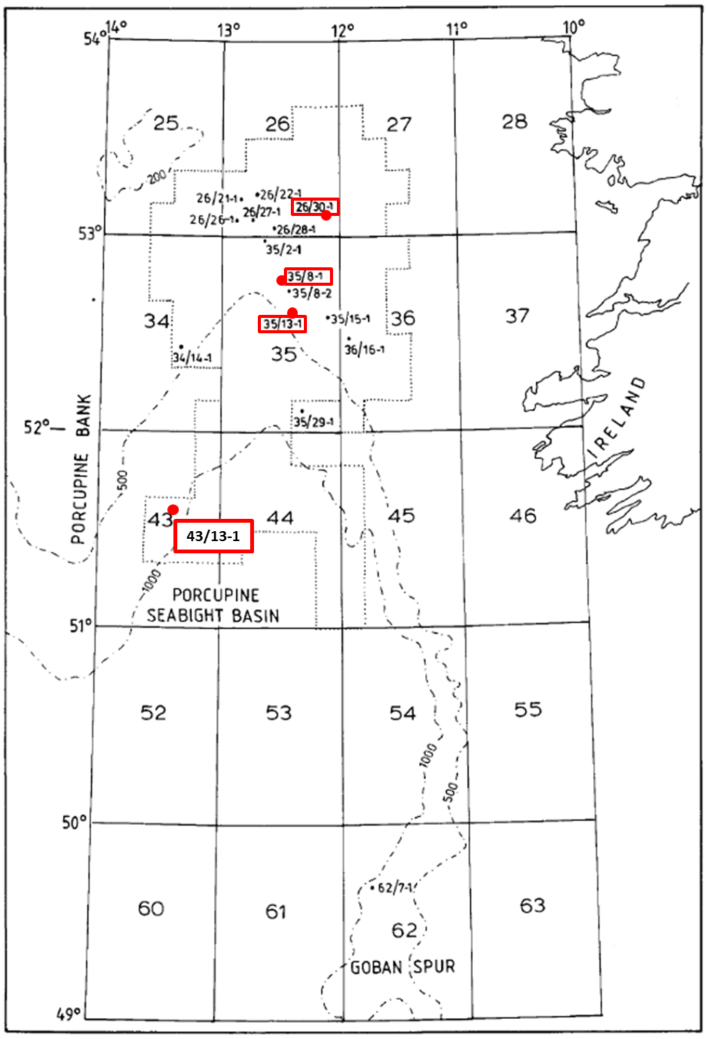

Fig. 15: Well locations in the Porcupine Basin adapted from Tate and Dobson (1989) with addition of well 43/13-1. Wells sampled in this study are highlighted with red boxes.

2.3.1) **35/8-1**

This study has sampled well 35/8-1 (near the NE margin of the Porcupine Basin) at 10668 ft. Robertson core log (Burley and Taylor, 1978) refers to a pumaceous tuff, intercalated with siltstone ca. 15 km from a vent, and overlain by Albian-Aptian marine sediments (Fig. 16). The report also interprets the ash deposit as water lain (deposited onto or into water). Intercalation with marine silts supports this. Core photos show a mainly monotonous pale grey-blueish tuffaceous lithology. Features, including laminations and grading, are consistent with water lain deposits (or at least indicate settling in water). However, these are difficult to identify in the core photographs. Some features appear to be eutaxitic to rheomorphic normally associated with high temperature compaction and flow of a hot volcanic deposit, although a marine environment is not ruled out. Ash layer was intruded by Cenozoic dolerite so it may be slightly metasomatised.

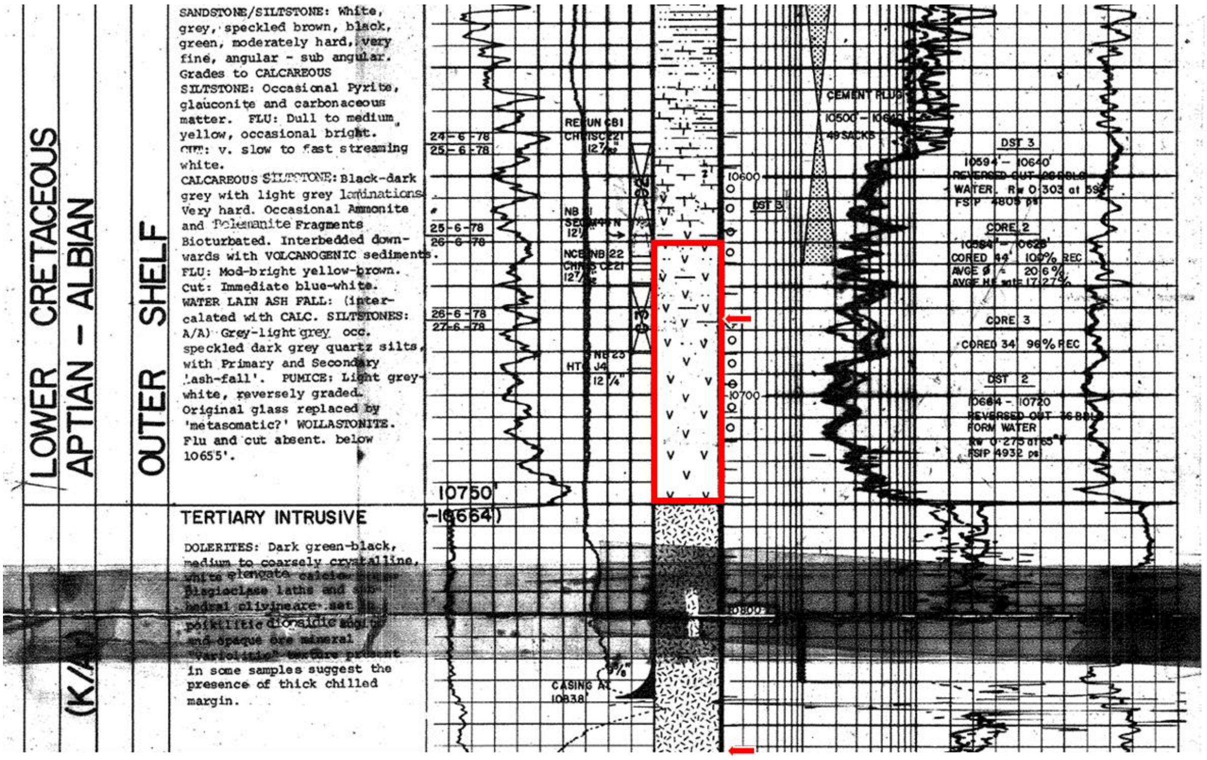

Fig. 16: Portion of the composite log for well 35/8-1. Volcanic horizon is highlighted. Sample taken in this study indicated by upper red arrow. Location of junk basket samples described by Burley and Taylor (1978) indicated by lower red arrow.

Petrographic description carried out as part of K-Ar dating on the mafic intrusion by Robertson (Burley and Taylor, 1978) interprets this horizon as a contact metamorphosed bedded tuff (junk basket at 10880 ft). This is close to the contact with dolerite. Two other samples from this level were of altered olivine basalt. All three samples are described as extensively altered. Prevalence of chlorite suggests high temperature and may be consistent with contact metamorphism and associated hydrothermal fluid flow. The tuff is described as devitrified volcanic glass consisting of pyroxene, biotite, epidote and secondary zeolite mainly filling fractures.

Sample at 10668 ft in this study (Fig. 16) appears to be pale (light grey) fine grained but speckled. Grey matrix with darker greenish 1-2 mm clots (Figs. 17A & C). It is a tuff comprised of medium-fine ash. The sample seems to have a low density when held in the hand (hence pumaceous) but this may also be from alteration to mainly clay. The sample has a chalky feel but it does not appear to be as altered as the description of Burley and Taylor (1978). It is useful to note the K-Ar age of 18.0 ± 0.6 Ma for the sample of olivine dolerite at 11090 ft. This could be usefully tested with Ar-Ar analysis of the sample from 10668 ft in this study.

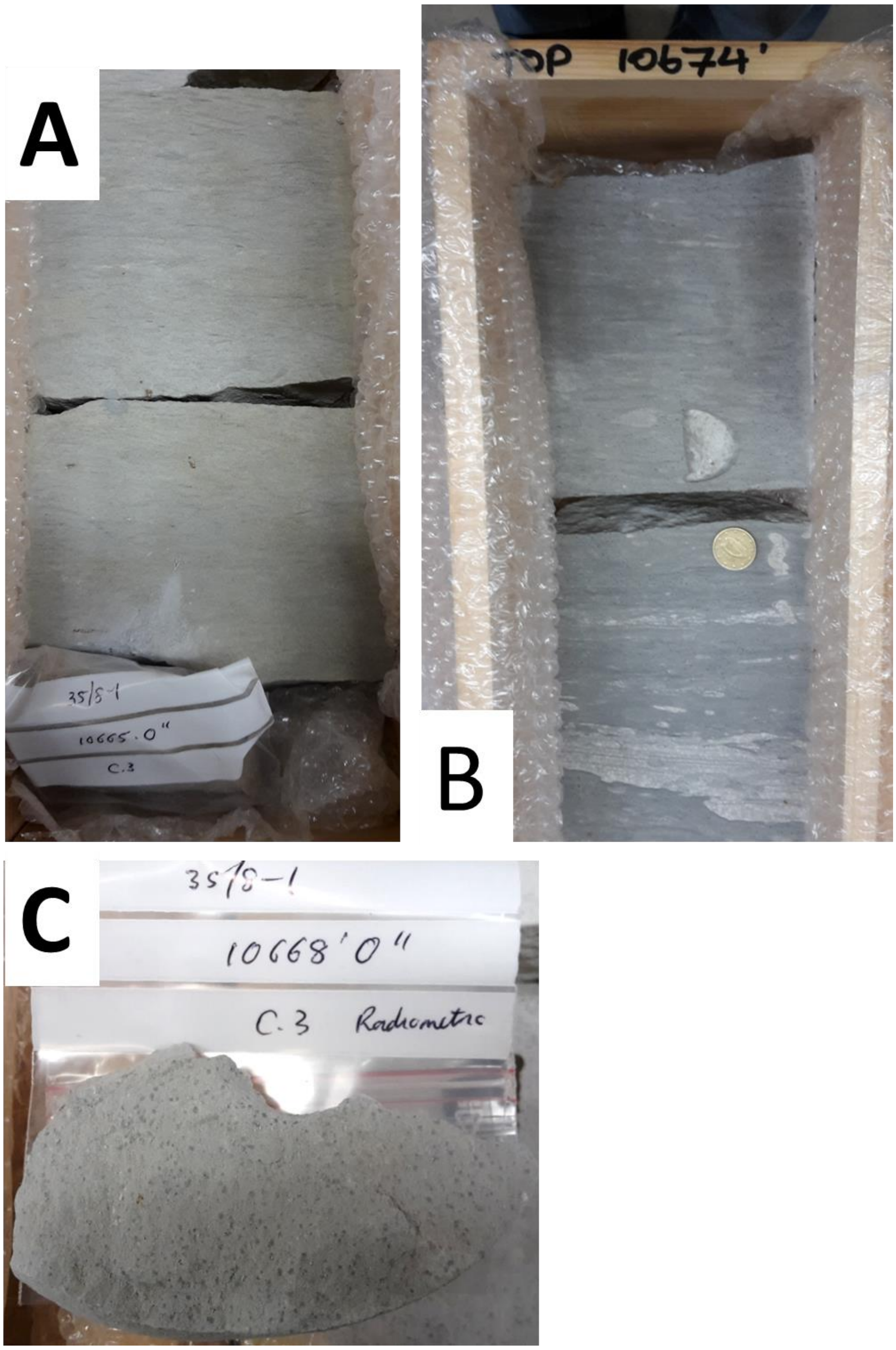

Fig. 17: Core photos from well 35/8-1 provided by P. Copestake (June 2017). A and C used in this study. B shows typical texture.

Thin section:

Quartz grains in feldspathic matrix (Fig. 18A). Patchy alteration to clay (chlorite and sericite) with darker microcrystalline clots (chlorite) (Fig. 18B). Occasional veins or irregular patches with fibrous zeolite.

Quartz grains are moderately sorted ranging from 0.01-0.1 mm and sub-rounded. Usually elongate or irregular and in detail show ragged or embayed margins and heavily included (Fig. 18C&D). Matrix/groundmass can be seen to be crystalline at high magnification. Difficult to identify feldspar (likely sanidine if not metasomatised) but a different refractive index to the quartz grains allows their distinction. There are also numerous but scattered and isolated needles of what is likely some kind of zeolite.

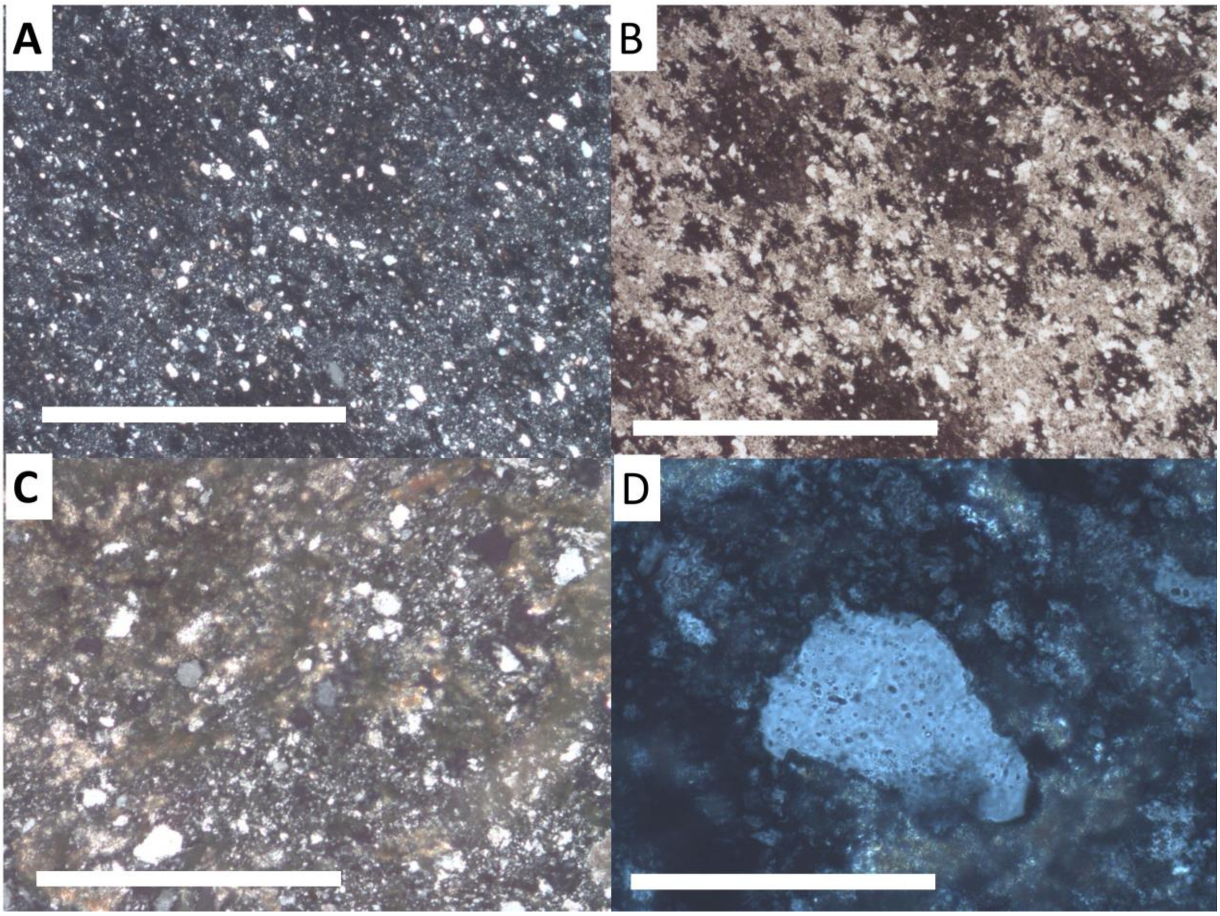

Fig. 18: Photomicrograph of sample from 35/8-1. A) Crossed polarised light, scale bar = 6 mm. Dominant texture is fine grained quartz in a mainly feldspathic matrix. Crystals too small to identify. Darker patches are dominated by clays. B) Plane polarised light, scale bar = 6 mm. Clay dominated patches are clearer in PPL. These may be relict fiamme. C) Crossed polarised light, scale bar = 2 mm. In detail, the quartz grains have irregular serrated and embayed margins, attesting to their volcanic origin. The amount of quartz present may be due to sorting in a marine (or at least aqueous) environment. D) Crossed polarised light, scale bar = 0.2 mm. Quartz grains are heavily included.

Environment of deposition is difficult to determine, but core samples showing lamination and the amount of quartz in thin section may be from aqueous or possibly marine deposition.

Dating recommendation: Ar-Ar whole rock analysis

2.3.2) **35/13-1A**

Well 35/13-1A near the northern end of the Porcupine Basin was sampled for this study at 3834.208m-3834.218m, near the upper boundary of a gabbro intrusion (sill) that intruded Lower Cretaceous sediments (Fig. 19). It has been suggested in the well log that this intrusion may be regionally extensive. Seemann (1984) reported a K-Ar age of Oligocene or older (25.8 ± 2.6 Ma) for the intrusion (although Seemann, 1984, did not mention the well name the location from this paper's location map is consistent with this well), but nearby well 35/8-1 has a K-Ar age of ca. 18 Ma (Miocene). It will be interesting if K-Ar on the tuff from 35/8-1 shows a younger age consistent with Oligocene or Miocene contact metamorphism. The ca. 25.8 Ma age was noted to be similar to a dyke that crops out onshore on the Dingle Peninsula that was dated as 25.6 ± 1.3 Ma by Horne and Macintyre (1975). The inference here is of some genetic link.

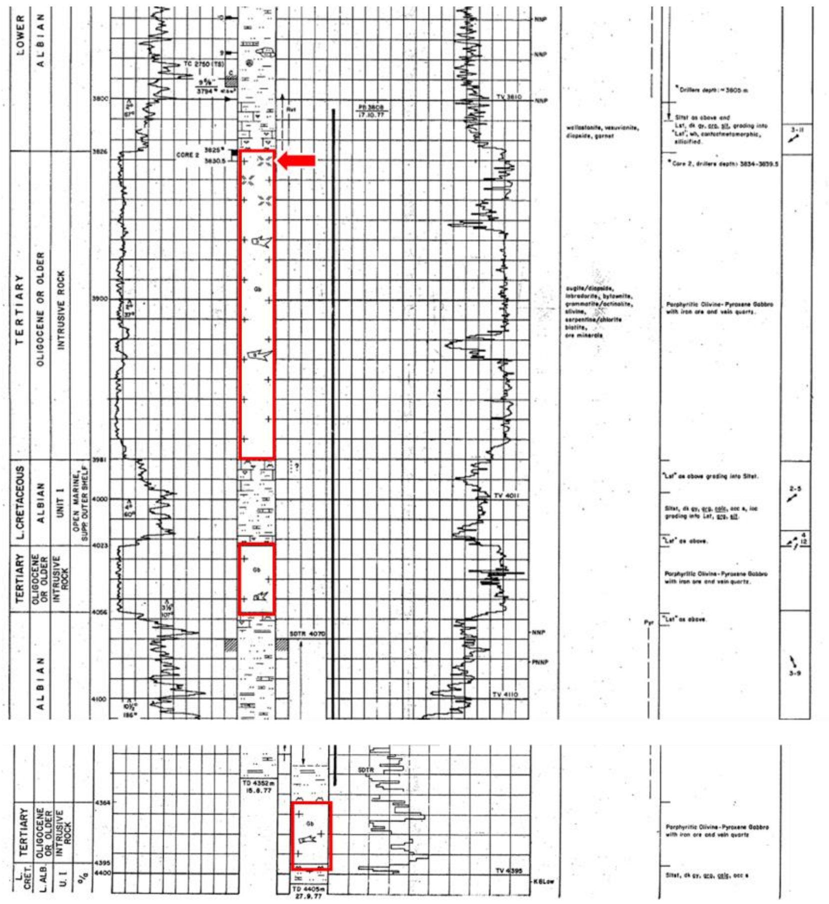

Fig. 19: Portion of composite log for well 35/13-1A. Gabbro is highlighted by red boxes showing three separate intrusions (NB. Gap in log 4110-4325 m). The sample used in this study indicated by red arrow near top of upper intrusion.

Existing core description details mineralogy consistent with slightly altered gabbro, but does not differentiate primary and secondary mineralisation. Main texture is a fine-grained matrix with ophitic feldspar-pyroxene intergrowth. Grammatite (tremolite), serpentinite and chlorite are likely secondary. Opaque mineral appear to be primary. Olivine is weakly serpentinised.

Sample is a fine-med dark greenish holocrystalline dolerite or microgabbro (Fig. 20). Plagioclase and pyroxene dominate with some olivine phenocrysts. Appears dark, but greenish colour likely indicates some alteration.

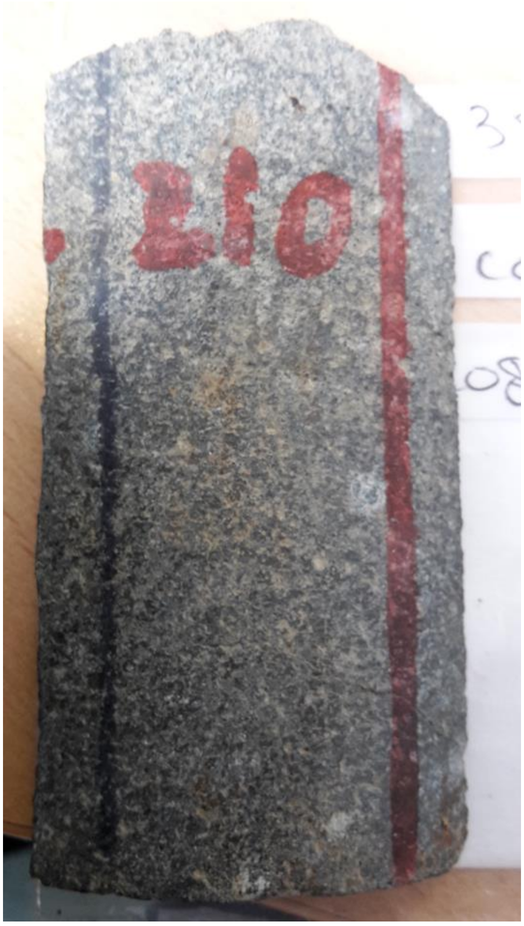

Fig. 20: Photo of core sample from well 35/13-1A used in this study.

Thin section:

Ophitic texture with clinopyroxene, and some orthopyroxene, ca. 1 mm with densely included with 0.1 mm laths plagioclase (Fig. 21). Olivine is either not obvious or is absent but there some very minor quartz and minor biotite. Alteration is moderate to high evident mainly from the presence of sericite and some chlorite. Plagioclase ca. 0.5 mm long and sparse 0.4 mm biotite for dating.

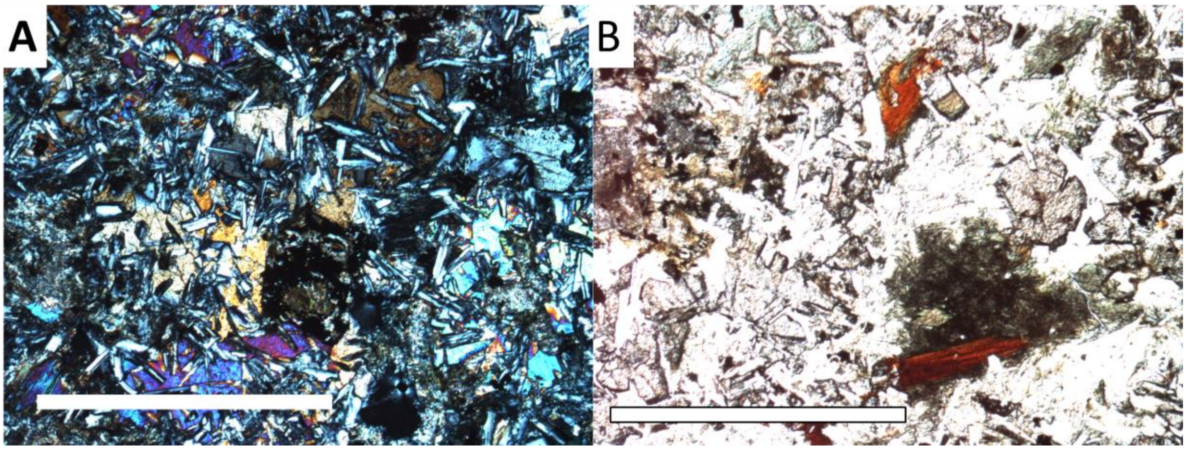

Fig. 21: Photomicrograph of sample from 35/13-1A. A) Crossed polarised light, scale bar = 2 mm. Ophitic texture with plagioclase laths scattered as inclusions in larger crystals of clinopyroxene. In addition, minor orthopyroxene is present. B) Plane polarised light, scale bar = 2 mm. Red-brown biotite, also greenish chlorite and some sericitisation.

Dating recommendation:

Ar-Ar on a mineral separates of plagioclase.

2.3.3) **43/13-1**

From well 43/13-1 in south Porcupine this study has collected ditch cuttings from two intervals; 2550-2560 m and 2590-2600 m. These cuttings are unwashed. The sample appears grey with large 10-15 mm clumps of consolidated mud and dust that both include white specs (0.1-0.2 mm). Clumps completely dissolve in water leaving rock fragments and white specs. Brown and Herbert (1988) reported basalt from cuttings at depths of 2628, 2615, 2612.5 and 2539.5 m. The basalt is described as variously light grey to dark grey with coarse feldspar phenocrysts in a heavily altered matrix. Alteration of the groundmass involves ferromagnesian silicate minerals, presumably pyroxene. Alteration to calcite and zeolites.

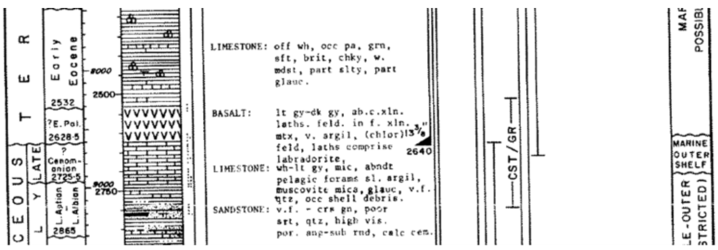

Interval 2532.0 - 2628.5 (?Early Palaeocene)

The top of this interval is picked on a very pronounced decrease in the gamma ray response together with a less pronounced increase in resistivity and sonic travel time. This boundary marks the top of a thick basalt pile.

Lithology: light to dark grey porphyritic basalt with abundant large phenocrysts of feldspar in a very fine crystalline matrix. Feldspar lathes comprise labradorite with broad albite - type twin lamellae (c. 40% of rock).

The rock commonly shows a chlorite green tinge due to the heavy alteration of the ferromagnesium silicate minerals.

Palaeoenviroment: ?Marine.

Fig. 22: Portion of well summary log for well 43/13-1 along with petrographic description from well report.

Samples were washed over a 500 µm sieve and air-dried.

- **43/13-1 2550-2560 m**

Fragments 0.1 -2 mm include very fine basalt (with some epidote), white specs (quite friable/crumbly – probably zeolite), bluish very fine-fine silt siltstone, red brown friable mudstone. Basalt and pale (bluish) silt predominate.

- **43/13-1 2590-2600 m**

Much as above but fewer white specs (zeolites). Fragments include fewer basaltic and more fine - grained sediments. Fragments are usually 1-2 mm rarely up to 10 mm and include dark (basaltic), red brown (mudstone), pale grey-green (siltstone) and some white zeolites.

Dating recommendation:

Some alteration but Ar-Ar on a chip selected from the cuttings is most likely to yield usable results.

2.3.4) **26/30-1**

Well report noted that the well bottomed out in granitic basement (Fig. 23). Above this is quartzite. The report also describes issues with lost circulation at 5994 ft with uncertainty over whether this was in overlying sandy layers or fractures at this depth. Cutting bag is dominated by mica from the drilling mud accordingly. Samples were washed over a 500 µm sieve and air dried.

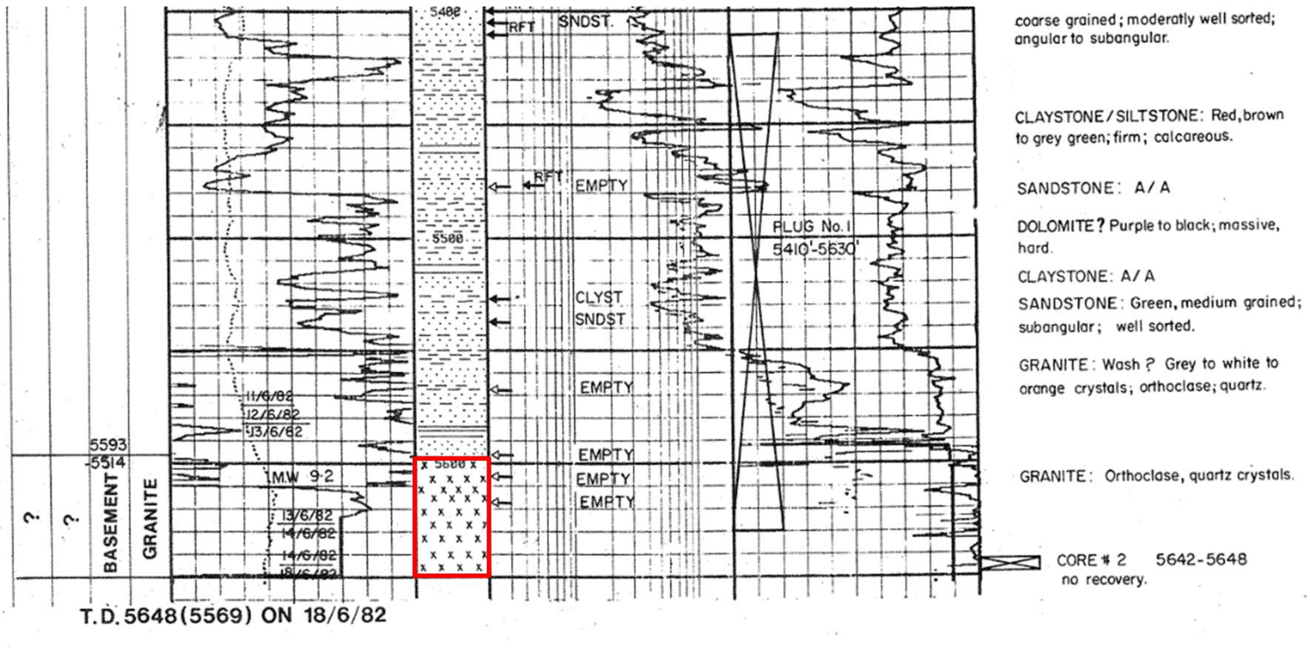

Fig. 23: Portion of core log for well 26/30-1 showing granite encountered at bottom (red box). Cuttings taken from bottom of the well.

- **26/30-1 5610'**

Washed cuttings include ca. 60% large clear mica flakes. Rock fragments 0.1-3 mm include K feldspar, quartz, biotite, ferromagnesian and plagioclase. Proportions seem to be consistent with a more alkali feldspar rich granitoid. Other rock fragments include very fine-fine silt bluish grey siltstone and dark red-brown friable mudstone. Latter possibly contributing to colouration of unwashed sample with drilling mud.

- **26/30-1 5620'**

Similar to above but less mica ca. 40-50%. More of the red-brown friable mudstone, ca. 10% in 0.5- 1 mm fragments. Rock fragments consistent with a monzogranite or possibly granodiorite with some k feldspar, quartz, bit more plagioclase, biotite and occasional ferromagnesian fragment (latter ca. 2-3 mm). As above possibly pick out granitoid components.

Dating recommendation: Ar-Ar on biotite flakes hand-picked from cuttings.

2.4 Goban Spur

The Goban Spur Basin is located at the intersection of the Celtic Sea basins and Porcupine Basin, the faulting array is complex (Shannon, 1991) (Fig. 24). In the Goban Spur area, to the south of the Porcupine fault (Dingle and Scrutton, 1979; Naylor and Shannon, 2005) dredging has revealed Upper Palaeozoic rocks comprising weakly metamorphosed sediment intruded by granite and likened to onshore Cornwall (Masson *et al.*, 1989; Naylor and Shannon, 2005). Rubidium-strontium and potassium-argon dating of granite samples yielded 275 Ma (total rock) and 290 Ma (biotite) ages indicating a Variscan, Early Permian intrusive episode here (Auffret *et al.*, 1979).

An important igneous episode occurred in Early Cretaceous time, represented by the Barra and Porcupine Volcanic Ridge systems. The Barra system remained upstanding until the Eocene, whereas the Porcupine system was onlapped and buried by mid-Cretaceous time (Bentley & Scrutton 1987; Scrutton & Bentley 1988). Jurassic volcanics have been reported from the neighbouring Celtic Sea basins by Kamerling (1979), Roberts *et al.* (1981) and Robinson *et al.* (1981).

This study has core sample from well 62/7-1.

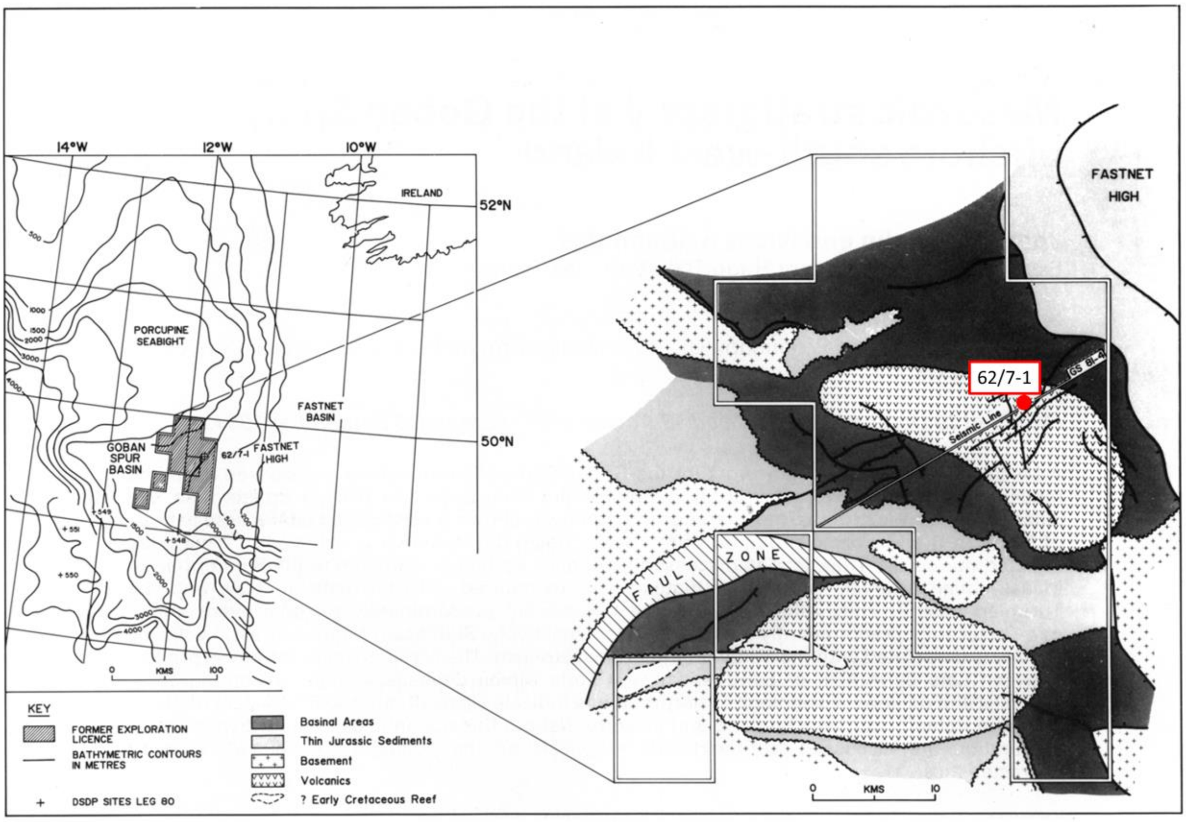

Fig. 24: Location and geology of Goban Spur area adapted from Colin *et al.*, (1992).

2.4.1) **62/7-1**

Colin *et al.* (1992) reported 200 m of porphyritic basalt interbedded with (including coal horizons) and overlain by Bathonian sandstone, Colin *et al.* (1992) also refer to radiometric dating that supports Bathonian age for the basalts. Tate and Dobson (1988) reported 207 m of porphyritic basalt in this well. The thickness is consistent with the 222 m recorded in the core log for this well. However, Tate and Dobson (1988) noted that the basalts overlie Bathonian-Callovian sediments and have been dated as 133 Ma (averaged from 130 ± 2 and 137 ± 2 Ma dates; Esso, pers. comm. 1987, in Tate and Dobson, 1988) which equates to Early Cretaceous (Hauterivian). Mark *et al*. (2009) carried out radiometric dating (based on Ar Ar analysis) of a sample from the well, however, this yielded an age of 93.8 +/- 1.0 Ma, which falls in the Turonian. Given the presence of biostratigraphically well dated Early Cretaceous sediments above the lava, this radiometric date is anomalous.

Tate and Dobson (1988) also reported geophysical wireline log data that supports an extrusive origin and petrographic and geochemical data indicating that the basalts are olivine-phyric tholeiites.

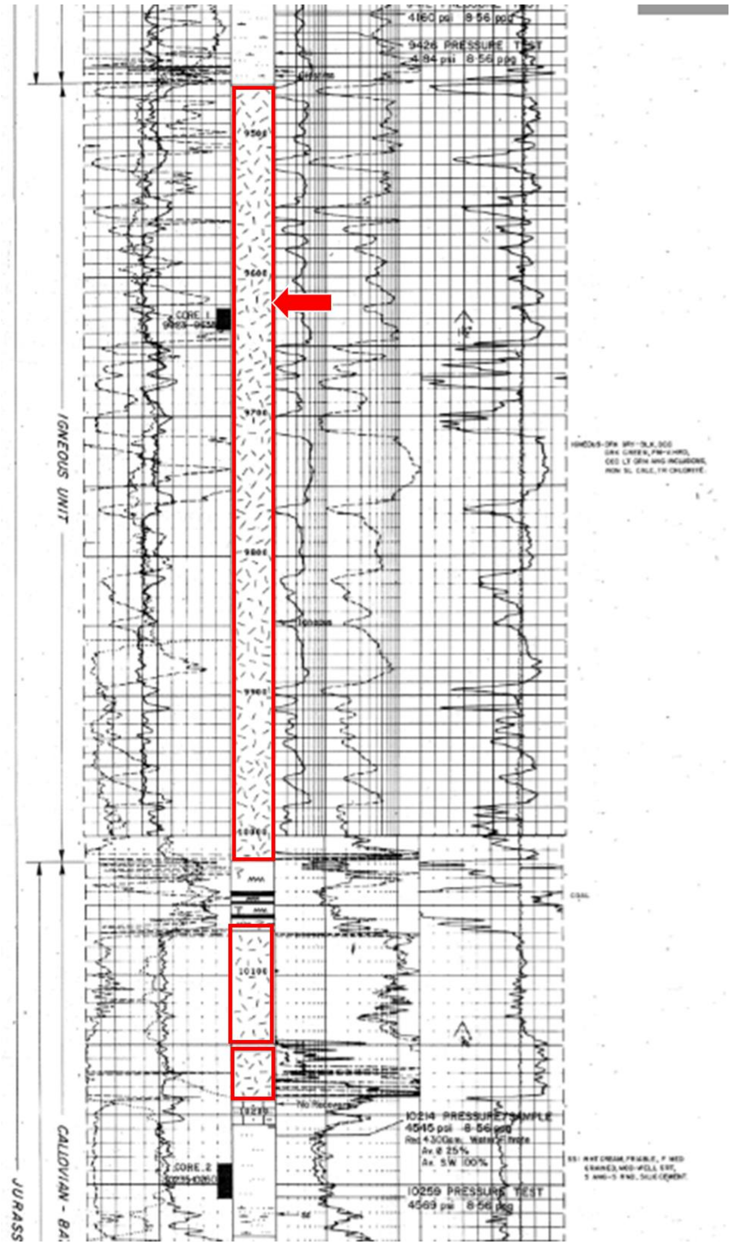

Fig. 25: Portion of core log for well 62/7-1. Basalt horizons are highlighted in red. Location of sample taken for this study indicated by red arrow.

Seismic evidence (Merlin interpreted seismic line; PAD 13-046M) seems to support a Jurassic age, given that the Base Cretaceous seismic horizon is interpreted above the lavas. This would agree with the Bathonian age proposed by Colin *et al.* (1992) and suggests there may be a genetic link with Fastnet volcanics. Other workers, do, however, place the Base Cretaceous seismic horizon below the lavas in 63/7-1.

The sample is a porphyritic basalt with a trachytic texture indicating trachybasalt or trachydacite (Fig. 26). The dominant features are large 2-10 mm size phenocrysts of white feldspar (plagioclase) in fine grained dark matrix. 10-15 mm spherical-irregular but always rounded inclusions of dark green/bluish aphinitc material. These may be amygdales filled with zeolite or possibly altered mafic enclave. Feldspars are variously square to lath shaped, some are quite euhedral and some show resorption. On a broken surface feldspars appear greenish yellow – epidote? There is a strong lamination that looks planar but it is difficult get an impression of this in 3D.

Fig. 26: Photo of core sample from well 62/7-1 provided by P. Copestake (June 2017).

Thin section:

Large plagioclase phenocrysts 2-3 mm up to 15 mm, variously euhedral and fragmental showing both complex zonation and concentric zonation (Fig. 27). Groundmass of 0.2-1 mm feldspar laths and altered pyroxene in what appears to be a mainly cumulate texture. Oxides distributed as small (c. 0.2 mm) crystals in groundmass. Amygdales (3-4 mm) filled with Si zeolite with brownish and greenish staining (these are filled vesicles and not xenoliths or enclaves – more consistent with extrusive setting).

Olivine is present in the groundmass but any larger phenocrysts of this and pyroxene seem to have been replaced by a deep red mineral (possibly some kind of oxyhydroxide). The red colour seems to mask birefringence and it is often rimmed by opaques.

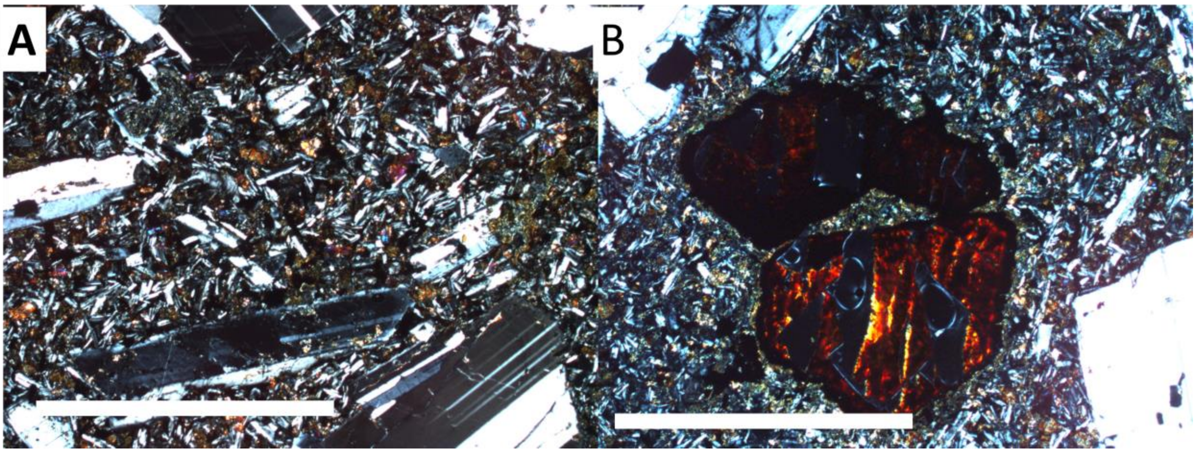

Fig. 27: Photomicrographs from sample 62/7-[illegible]. A) Crossed polarised light, scale bar = 2 mm. Porphyritic texture with large partly fragmental plagioclase phenocrysts showing a variety of zoning patterns. Groundmass is fine – medium grained plagioclase laths with pyroxene and olivine (latter now mostly replaced) and some clay (alteration). B) Crossed polarised light, scale bar = 1 mm. Red secondary mineral (red colour masks birefringence) with greenish alteration halo likely of fine chlorite in the groundmass.

Dating recommendation:

Some uncertainty over age in literature. It is possible a K-Ar date could have suffered Ar loss due to later hydrothermal alteration. There is opportunity to obtain a good date from feldspar phenocrysts or groundmass. Groundmass partly altered but more likely to yield a crystallisation age on eruption so would need a date from phenocrysts and groundmass separately. However, recommendation is to prioritise phenocrysts.

2.5 Fastnet Basin

The Fastnet Basin is a NE-SW trending fault bounded basin that extends SW from the Celtic Sea basin (Caston *et al.*, 1981; Shannon, 1991) (Fig. 28). Three wells (56/26-1, 56/26-2 and 64/2-1, Fig. 28B) in this basin penetrated olivine microgabbro/dolerite that have yielded 170 ± 4 Ma (Middle Jurassic, Bajocian) from K-Ar dating (Caston *et al.*, 1981). The sills intruded Lower Jurassic (Hettangian-Sinemurian) sediments. Caston *et al.*, (1981) described six sills and three igneous plugs from these three wells and 2D seismic data. The descriptions of the sills are vague and it would be interesting to see if any more recent or reprocessed seismic data exists. Some descriptions of doming of sediments may be related to forced folds or hydrothermal vents (e.g. Magee *et al.*, 2014, 2015). Forced folds may help with dating of intrusions from sediments that onlap these folds.

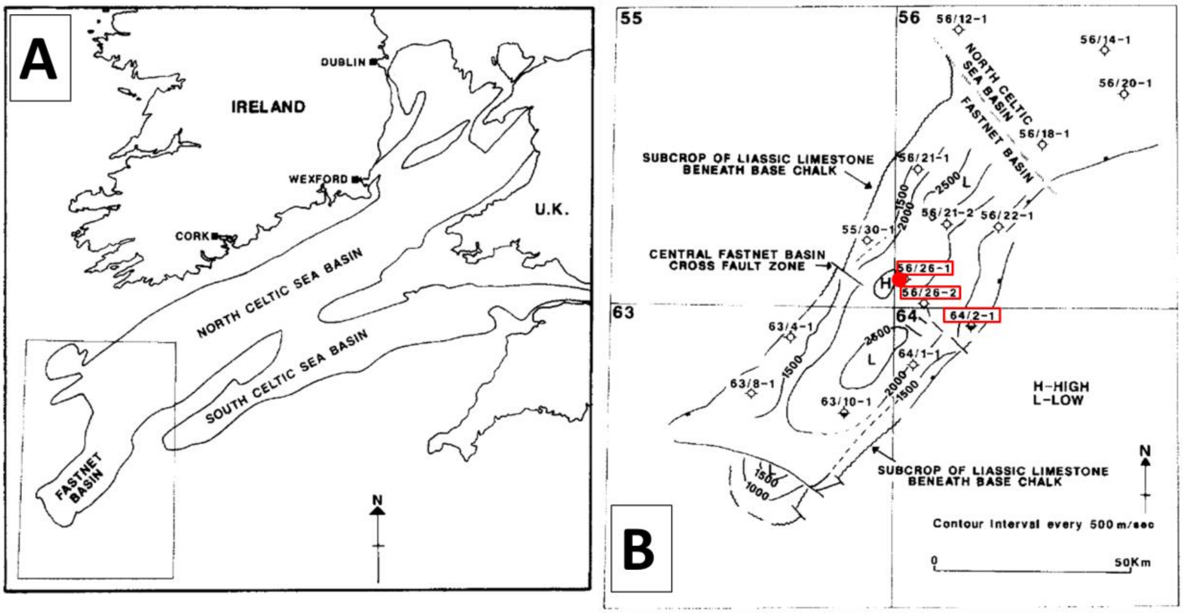

Fig. 28: Adapted from Murphy and Ainsworth (1991). A) Location map the Fastnet Basin. B) Location of wells in the Fastnet Basin. Wells mentioned in text highlighted with red boxes and well sampled in this study with a red dot.

From Caston *et al.*, (1981):

> 'BP 56/26-1. This well penetrated an olivine-microgabbro sill between 2888.5 m and its total depth (TD) at 2931 m. The bottom of the sill was not reached. The gabbro underlay a sand and shale sequence of lower Liassic (probably Sinemurian-Hettangian) age. Evidence of thermal metamorphism was noted in cuttings and sidewall cores within a 40 m thick zone overlying the sill.
>
> BP 56/26-2. This passed through 3 olivine-dolerite sills (Fig. 2), of which the thickest is 42.5 m. These are intruded into a sand-shale sequence, dated on sparse palynoflora and microfauna as Sinemurian to Hettangian. Mineralogical effects of thermal metamorphism occur in cuttings from 2330 to 2465 m, but carbonization of palynoflora occurs from 2175 to 2566 m. The top of the underlying Liassic Limestone (terminology of Robinson et al, 1980) occurs at 2566.5 m.

Elf 64/2-1. This penetrated a single 86 m thick sill between 1482 and 1568 m, intruded in the Lias Limestone, the top of which occurs at 1241 m. Little evidence of thermal metamorphism was recorded from cuttings during the drilling of the well; however, no in situ palynomorphs were recovered between 1440 and 1625 m because of thermal effects in the vicinity of the sill. 2 other wells, Elf 55/30-1 and Deminex 56/21-1, both drilled to the pre-Jurassic, did not penetrate igneous material. The third well, Deminex 56/21-2 (Fig. 3), also failed to penetrate a sill, but nevertheless recorded a 45 m thick silicified zone accompanied by extensive mineralization within the Lias Limestone.'

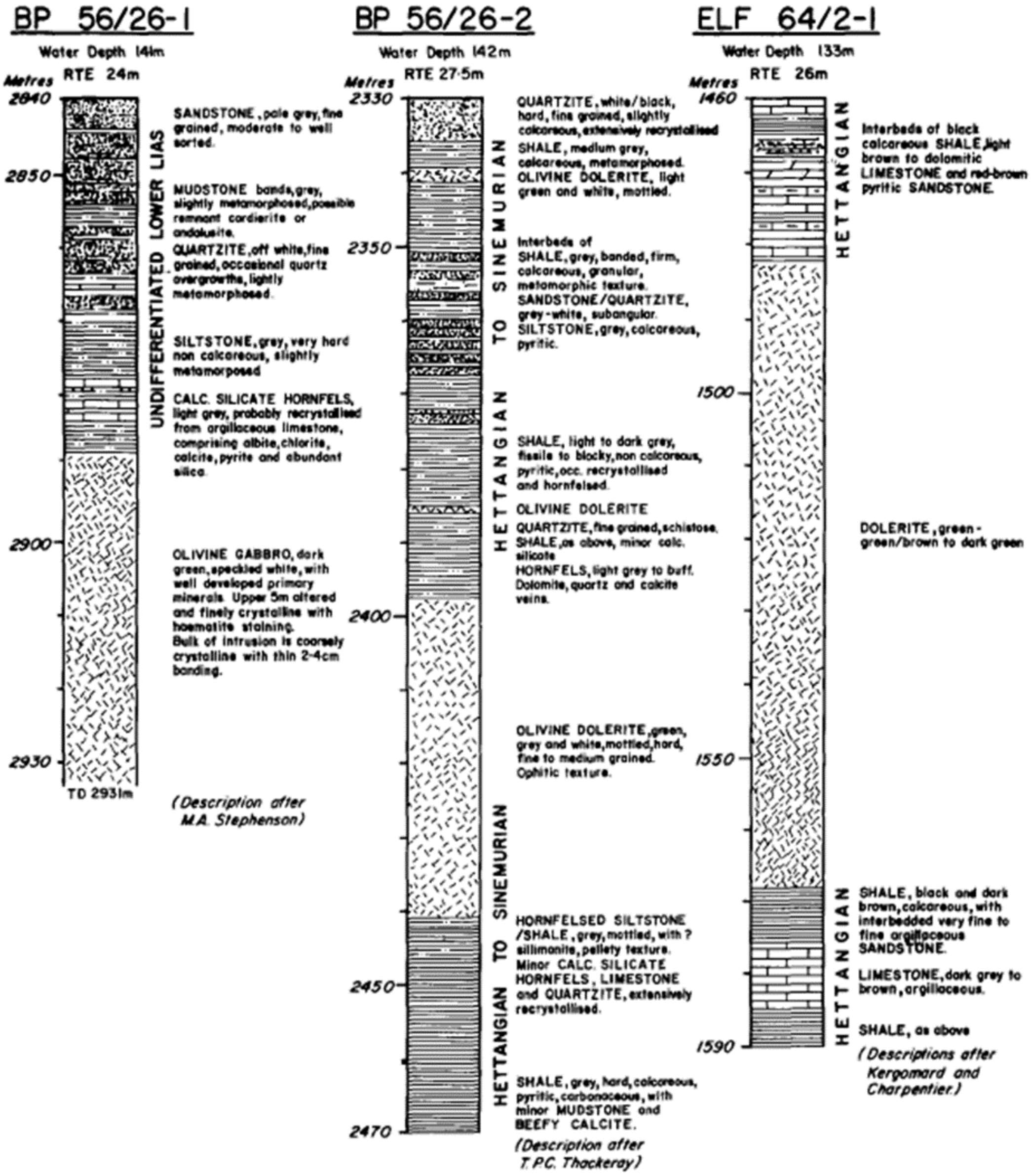

Fig. 29: Reproduced from Caston *et al.*, (1981) Fig. 2, showing portions of core logs from three wells (highlighted in Fig. 28) that penetrated microgabbro sills.

The top Bajocian in this well is an unconformity at 1342m, which is overlain by Lower Cretaceous Greensands (Wealden facies). The top of the sill is 2888.5 m giving an emplacement depth of 1546.5

m. This is similar to emplacement depth of the Golden Valley Sill, Karoo, South Africa (Schofield *et al.*, 2010). This depth would allow fluidisation of country rocks and may facilitate hydrothermal venting and saucer shaped sills.

Detailed description from Caston *et al.*, (1981) of microgabbro in 56/26-1:

> 'holocrystalline micro gabbro with a framework of plagioclase laths (averaging 0.6X 0.06 mm), olivine crystals (up to 1.5 mm) set in anhedral plates (up to 4.0 mm) of pale-brown clinopyroxene which form poikilophitic growths with partly sericitized feldspar laths. Accessory hornblende may enclose olivine; there are minor partly chloritized mica, granules of magnetite, ilmenite and traces of apatite and zircon. There is rare interstitial analcime, indicating a slight alkali residuum, and prehnite. The modal composition is: labradorite (with alteration products) 45%, olivine 30%, clinopyroxene 20%, biotite 3%, hornblende <1%, opaque iron-titanium oxide <1%, secondary minerals including mica, chlorite, analcime, prehnite 1%.'

2.5.1) **56/26-1**

Sample appears as a medium-coarse grained, weakly porphyritic (phaneritic holocrystalline), orthocumulate gabbro (Fig. 30). Hand specimen shows fairly euhedral 3-5 mm laths of plagioclase that appear to be fresh. Groundmass is dominated by sub-millimetre scale phenocrysts of mainly hornblende, pyroxene, feldspar and olivine. No obvious quartz and no obvious fabric. Some bronze coloured patches, possibly secondary mica also some minor alteration or iron (ilmenite) staining.

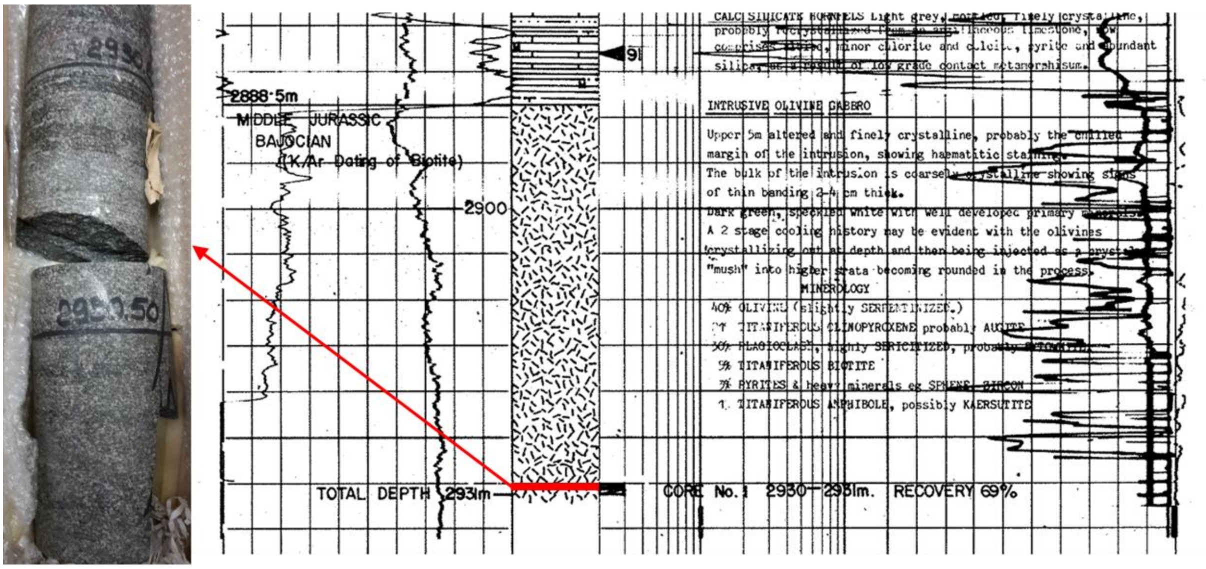

Fig. 30: Core photo (left) provided by P. Copestake (June 2017) of sample taken from this study from well 56/26-1. Right, portion of core log showing location of sample.

Thin section:

Clinopyroxene, orthopyroxene, olivine, biotite, oxide, chlorite, sericite. Coarse grain size generally typically 0.5-2 mm. Ophitic pyroxene (c. 5 mm) with plagioclase and olivine. Both clinopyroxene and orthopyroxene present (Fig. 31). Also patches of cumulate texture dominated by feldspar with less pyroxene. Olivine distributed throughout roughly consistently. Opaques form either as small inclusions in pyroxene phenocrysts but are mainly replacing biotite. Alteration is moderate with chlorite replacing pyroxene and sericite replacing feldspar.

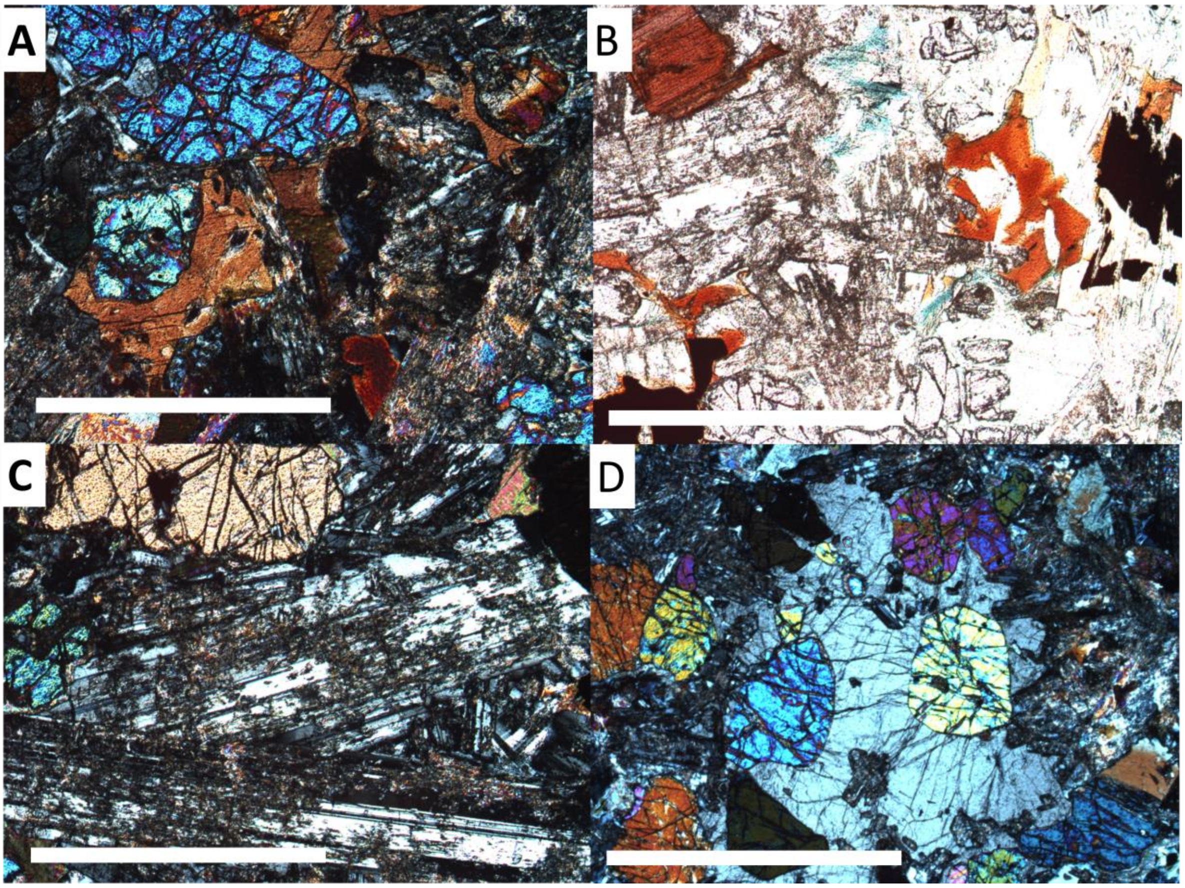

Fig. 31: Photomicrographs from sample 56/26-1. A) Crossed polarised light, scale bar = 2 mm. Olivine, and interstitial biotite with replaced feldspars. Cumulate texture. B) Plane polarised light, scale bar = 2 mm. Biotite and chlorite clear. C) Crossed polarised light, scale bar = 2 mm. Moderately sericitised plagioclase feldspar. D) Crossed polarised light, scale bar = 2 mm. Ophitic pyroxene with olivine.

Dating recommendation:

Already has K-Ar biotite date but worth obtaining Ar-Ar on plagioclase mineral separate.

3. References

Auffret, G.A., Pastouret, L., Cassat, G., De Charpal, O., Cravatte, J. and Guennoc, P., 1979. Dredged rocks from the Armorican and Celtic margins. *Initial Reports of the Deep Sea Drilling Project*, *68*, pp.473-491.

Bentley, P.A.D., and Scrutton, R.A., (1987) Seismic investigations into the basement structure of southern Rockall Trough. In: Petroleum Geology of Northwest Europe (Eds J. Brooks and K. W. Glennie), Graham and Trotman, London, pp. 667-675

Brown, J., and Herbert, G., 1988. Ireland: Porcupine Basin well 43/13-1 geological completion report. Report No. DUB 1363.

Burley, S.D., Taylor, A.M., 1978. Potassium-Argon age dating and petrographic analysis of selected samples from the Phillips Petroleum Company 35/8-1 well. Offshore Ireland. Report No. 4214P. Project No. RRPS/789/C/2802Robertson Research International Ltd. Prepared for Phillips Petroleum (UK).

Caston, V.N.D., Dearnley, R., Harrison, R.K., Rundle, C.C. and Styles, M.T., 1981. Olivine-dolerite intrusions in the Fastnet Basin. *Journal of the Geological Society*, *138*(1), pp.31-46.

Colin, J.P., Ioannides, N.S. and Vining, B., 1992. Mesozoic stratigraphy of the Goban Spur, offshore south-west Ireland. *Marine and Petroleum Geology*, *9*(5), pp.527-541.

Chambers, L., Kempton, P., Hitchen, K. 2005. Geochemical and isotopic results for samples from the offshore region to the west of Ireland. *British Geological Survey BGS Commissioned Report*, CR/05/116. 22pp.

Dancer, P.N., Algar, S.T. and Wilson, I.R., 1999, January. Structural evolution of the Slyne Trough. In *Geological Society, London, Petroleum Geology Conference series* (Vol. 5, No. 1, pp. 445-453). Geological Society of London.

Dingle, R.V. and Scrutton, R.A., 1979. Sedimentary succession and tectonic history of a marginal plateau (Goban Spur, southwest of Ireland). *Marine Geology*, *33*(1-2), pp.45-69.

Doré, A.G., Lundin, E.R., Jensen, L.N., Birkeland, Ø., Eliassen, P.E. and Fichler, C., 1999, January. Principal tectonic events in the evolution of the northwest European Atlantic margin. In *Geological society, London, petroleum geology conference series* (Vol. 5, No. 1, pp. 41-61). Geological Society of London.

Funck, T., Geissler, W.H., Kimbell, G.S., Gradmann, S., Erlendsson, Ö., McDermott, K. and Petersen, U.K., 2016. Moho and basement depth in the NE Atlantic Ocean based on seismic refraction data and receiver functions. *Geological Society, London, Special Publications*, *447*, pp.SP447-1.

Haughton, P., Praeg, D., Shannon, P., Harrington, G., Higgs, K., Amy, L., Tyrrell, S. and Morrissey, T., 2005.. First results from shallow stratigraphic boreholes on the eastern flank of the Rockall Basin, offshore western Ireland. In *Geological Society, London, Petroleum Geology Conference series* (Vol. 6, No. 1, pp. 1077-1094). Geological Society of London.

Horne, R.R. and Macintyre, R.M., 1975. Apparent age and significance of Tertiary dykes in the Dingle Peninsula, SW Ireland. Royal Dublin Society.

Kamerling, P., 1979. The geology and hydrocarbon habitat of the Bristol Channel Basin. *Journal of Petroleum Geology*, *2*(1), pp.75-93.

Kelley, S., 2002. K-Ar and Ar-Ar dating. *Reviews in Mineralogy and Geochemistry*, *47*(1), pp.785-818.

Lucas, P.M., (2004), Well 12/2-1z, Offshore Western Ireland: Reservoir Geological Study of the Pre-Cretaceous Interval. Report No. 8697/Id, Project No. Id/GF242. Roberton Research International Ltd. Prepared for Enterprise Energy Ireland Ltd.

Magee, C., Jackson, C.L. and Schofield, N., 2014. Diachronous sub-volcanic intrusion along deep-water margins: Insights from the Irish Rockall Basin. *Basin Research*, *26*(1), pp.85-105.

Magee, C., Maharaj, S.M., Wrona, T. and Jackson, C.A.L., 2015. Controls on the expression of igneous intrusions in seismic reflection data. *Geosphere*, *11*(4), pp.1024-1041.

Mark, D., Millar, I. L. and Hitchen, K. 2009. Geochronology of volcanic rocks from the Irish Shelf. *British Geological Survey, Marine Geoscience Programme Commissioned Report* CR/09/018.

Masson, D.G., Dobson, M.R., Auzende, J.M., Cousin, M., Coutelle, A., Rolet, J. and Vaillant, P., 1989. Geology of Porcupine Bank and Goban Spur, Northeastern Atlantic—Preliminary results of the Cyaporc submersible cruise. *Marine geology*, *87*(2-4), pp.105-119.

Naylor, D. and Shannon, P.M., 2005, January. The structural framework of the Irish Atlantic Margin. In *Geological Society, London, Petroleum Geology Conference series* (Vol. 6, No. 1, pp. 1009-1021). Geological Society of London.

Roberts, D.G., Masson, D.G., Montadert, L. and De Charpal, O., 1981. Continental margin from the Porcupine Seabight to the Armorican marginal basin. *Petroleum geology of the continental shelf of north-west Europe*, *1*, pp.455-473.

Robinson, K.W., Shannon, P.M. and Young, D.G.G., 1981. The Fastnet Basin: an integrated analysis. *Petroleum geology of the continental shelf of north-west Europe. Heyden, London*, pp.444-454.

Seemann, U., 1984. Tertiary intrusives on the Atlantic continental margin off southwest Ireland. *Irish journal of earth sciences*, pp.229-235.

Schofield, N., Stevenson, C. and Reston, T., 2010. Magma fingers and host rock fluidization in the emplacement of sills. *Geology*, *38*(1), pp.63-66.

Schofield, N.J., Brown, D.J., Magee, C. and Stevenson, C.T., 2012. Sill morphology and comparison of brittle and non-brittle emplacement mechanisms. *Journal of the Geological Society*, *169*(2), pp.127-141.

Scrutton, R.A. and Bentley, P.A.D., 1988. Major Cretaceous volcanic province in southern Rockall Trough. *Earth and Planetary Science Letters*, *91*(1-2), pp.198-204.

Shannon, P.M., 1991. The development of Irish offshore sedimentary basins. *Journal of the Geological Society*, *148*(1), pp.181-189.

Stoker, M.S., Stewart, M.A., Shannon, P.M., Bjerager, M., Nielsen, T., Blischke, A., Hjelstuen, B.O., Gaina, C., McDermott, K. and Ólavsdóttir, J., 2016. An overview of the Upper Palaeozoic–Mesozoic stratigraphy of the NE Atlantic region. *Geological Society, London, Special Publications*, *447*, pp.SP447-2.

Tate, M.P. and Dobson, M.R., 1989. Pre-Mesozoic geology of the western and north-western Irish continental shelf. *Journal of the Geological Society*, *146*(2), pp.229-240.

Tate, M.P. and Dobson, M.R., 1988. Syn-and post-rift igneous activity in the Porcupine Seabight Basin and adjacent continental margin W of Ireland. *Geological Society, London, Special Publications*, *39*(1), pp.309-334.

4. Appendices

Appendix 1: Summary dating recommendations

Sample	***Area (rock type)***	***Dating remarks***	***Recommendation***	***Sample weight***
56/26-1 2930.55 m	Fastnet (gabbro)	Already has K-Ar biotite date. Probably worth repeating on biotite and plagioclase or Ar-Ar on plagioclase	Ar-Ar On plagioclase separate as a priority. 1 analysis incl. mineral separation	195 g
35/13-1A, 3834.21-3834.22 m	Porcupine (gabbro)	K-Ar on biotite or plagioclase but risk of spurious date from alteration. Ar-Ar probably produce more reliable date	Alteration is moderate so Ar-Ar may provide a more reliable date. Plagioclase separate as priority 1 analysis incl. mineral separation	80 g
62/7-1 **2934.31 m**	Goban Spur (porphyrytic basalt)	Some uncertainty over age in literature. Opportunity to obtain good date from feldspar phenocrysts by Ar-Ar. Groundmass partly altered	Due to uncertainty that K-Ar might not resolve, Ar-Ar on plagioclase phenocrysts and groundmass would more likely allow resolution of age uncertainty. Prioritise plagioclase phenocrysts 1 analyses Ar-Ar incl. mineral separation	195 g
19/13-sb02 (BH1A) 106.4m	Slyne Basin (lava)	Fine grained and moderately altered so whole rock	Moderate alteration effect on K-Ar date might be overcome with Ar-Ar 1 analysis whole rock	60 g
12/2-1z 3963.6 m	Dooish, Rockall (altered basalt)	Some metasomatic feldspar might give a date at least close to emplacement. Whole rock date on a chip	Riskiest sample regardless of technique. Although Ar-Ar might distinguish hydrothermal event	

		from matrix	from emplacement, the emplacement (crystallisation) may not be datable. 1 analysis, Ar-Ar incl. mineral seperation	
12/2-1z 3963.0 m	Dooish, Rockall (basalt breccia)	No dating recommended		200 g
12/2-1z 3962.81 m	Dooish, Rockall (basalt breccia)	No dating recommended		95 g
16/28-sb01 147.76 m	Rockall (basalt)	Try to obtain date from plagioclase.	Ar-Ar may be able to distinguish crystallisation from subsequent alteration. Target plagioclase separate 1 analyses incl. mineral separation	180 g
16/28-sb01 148.25 m	Rockall (basalt)	Try to obtain date from plagioclase.	Ar-Ar may be able to distinguish crystallisation from subsequent alteration. Target plagioclase separate 1 analyses incl. mineral separation	190 g
35/8-1 **10668' (3251.6 m)**	Porcupine (tuff)	Ar-Ar or possibly U-Pb on zircon or monazite (if present)	Whole rock Ar-Ar1 analysis whole rock	140 g
26/30-1 5610' (1709.93	North Porcupine (basement	Ar-Ar on biotite or k-spar	Use sample 5620' as has less vermiculite (no	

m)	granite)granite		dating recommended)	
26/30-1 5620' (1712.98 m)	North Porcupine (basement granite)	Ar-Ar on biotite or k-spar	Ar-Ar on feldspar picked from cuttings	
43/13-1 2550-2560 m	Porcupine (basalt)	Ar-Ar whole rock on chip	Ar-Ar whole rock on chip selected from cuttings	
43/13-1 2590-2600 m	Porcupine (basalt)	Ar-Ar whole rock on chip	Use sample 2550-2560 m as has less zeolite (no dating recommended)	

For all dating recommendations, the priority is to target feldspar when a mineral separation is required. If suitable feldspar cannot be obtained then revert to mica.

When no mineral separation is recommended, the assumption is for whole rock if not otherwise stated.

Appendix 2: List of Photomicrographs from core samples

Well	sample	File name	XPL/ PPL	Field of view	Brief description
12/2-1z	3962.81 m	SNAP-155808-0020.jpg	XPL	6 mm	Calcite vein and replacement textures
		SNAP-160923-0030.jpg	XPL	6 mm	Calcite vein and replacement textures
	3963.0 m	SNAP-154647-0014.jpg	XPL	6 mm	Composite vein
		SNAP-154831-0015.jpg	PPL	6 mm	Composite vein
		SNAP-154930-0016.jpg	XPL	6 mm	Spar calcite
		SNAP-155208-0017.jpg	XPL	6 mm	Replacement textures
		SNAP-155341-0018.jpg	PPL	4 mm	Relict phenocrysts
		SNAP-155537-0019.jpg	XPL	6 mm	zeolites
		SNAP-155919-0021.jpg	XPL	6 mm	Composite vein
		SNAP-155950-0022.jpg	XPL	6 mm	Calcite and staining
		SNAP-160038-0023.jpg	XPL	6 mm	Composite vein
	3963.6 m	SNAP-173227-0006.jpg	XPL	6 mm	Composite inclusion fill
		SNAP-173332-0007.jpg	XPL	6 mm	feldspars
		SNAP-173426-0008.jpg	PPL	6 mm	texture
		SNAP-173640-0009.jpg	PPL	6 mm	Coarse calcite
		SNAP-174220-0010.jpg	XPL	2 mm	Detail inclusion fill
16/28-sb01	147.6	SNAP-161451-0033.jpg	XPL	4 mm	Amygdale zeolite
		SNAP-161520-0034.jpg	XPL	6 mm	porphyritic
		SNAP-161533-0035.jpg	XPL	6 mm	Composite vein
		SNAP-161637-0036.jpg	XPL	4 mm	zeolite
		SNAP-161927-0037.jpg	XPL	6 mm	porphyritic
		SNAP-162031-0038.jpg	PPL	6 mm	Red mineral
	148.25	SNAP-162115-0039.jpg	XPL	6 mm	Porphyritic and replaced
		SNAP-162158-0040.jpg	XPL	6 mm	Amygdale halo
		SNAP-162221-0041.jpg	PPL	4 mm	Opaque interstitial
		SNAP-162244-0042.jpg	XPL	6 mm	Composite vein
		SNAP-162327-0043.jpg	PPL	4 mm	Opaque grains
		SNAP-162418-0044.jpg	XPL	4 mm	Opaque grains
		SNAP-162535-0045.jpg	XPL	2 mm	Detail amygdale zeolite
19/13-sb02 (BH1A)		SNAP-153633-0012.jpg	XPL	2 mm	Fine texture and red staining
		SNAP-153726-0013.jpg	PPL	2 mm	Texture and opaque
		SNAP-160615-0026.jpg	XPL	2 mm	microphenocrysts
		SNAP-161048-0031.jpg	XPL	1 mm	Needles zeolite and opaque
		SNAP-161154-0032.jpg	XPL	4 mm	Fine texture
35/8-1		SNAP-171347-0001.jpg	XPL	2 mm	Quartz and clays
		SNAP-172114-0002.jpg	XPL	4 mm	Clay patches

	SNAP-172845-0003.jpg	XPL	4 mm	Clay patches
	SNAP-172938-0004.jpg	PPL	4 mm	Clay patches
	SNAP-173107-0005.jpg	XPL	1 mm	Included quartz
35/13-1A	SNAP-151905-0006.jpg	XPL	6 mm	Ophitic texture
	SNAP-152204-0007.jpg	XPL	6 mm	Some replacement
	SNAP-152334-0008.jpg	PPL	6 mm	biotite
56/26-1	SNAP-145831-0001.jpg	XPL	6 mm	Olivine and biotite
	SNAP-145932-0002.jpg	PPL	6 mm	Biotite
	SNAP-150131-0003.jpg	XPL	6 mm	Moderately sericitised feldspar
	SNAP-150355-0004.jpg	PPL	4 mm	Biotite, opaque and some chlorite
	SNAP-150815-0005.jpg	XPL	6 mm	Pyroxene and olivine
	SNAP-160450-0024.jpg	XPL	6 mm	Pyroxene and olivine
	SNAP-160517-0025.jpg	PPL	6 mm	Biotite, opaque and some chlorite
62/7-1	SNAP-152726-0009.jpg	XPL	4 mm	Porphyritic texture
	SNAP-153146-0010.jpg	XPL	2 mm	Red replacement mineral
	SNAP-153224-0011.jpg	PPL	2 mm	Red replacement mineral
	SNAP-160735-0027.jpg	XPL	4 mm	Porphyritic and alteration
	SNAP-160759-0028.jpg	XPL	2 mm	Red replacement mineral
	SNAP-160820-0029.jpg	PPL	2 mm	Red replacement mineral

Appendix 3: Photomicrographs

[see attached files]